EFFECTS OF SPIRAL LONGITUDINAL VORTICES ON TURBULENT BOUNDARY LAYER SKIN FRICTION

by J. G. Spangler and C. S. Wells, Jr.

Prepared under Contract No. NASw-956 *by*
LING-TEMCO-VOUGHT, INC.
Dallas, Tex.
for

NATIONAL AERONAUTICS AND SPACE ADMINISTRATION • WASHINGTON, D. C. • DECEMBER 1964

EFFECTS OF SPIRAL LONGITUDINAL VORTICES ON TURBULENT BOUNDARY LAYER SKIN FRICTION

By Jack G. Spangler and C. Sinclair Wells, Jr.

SUMMARY

12502

As a part of an experimental investigation of the effects of ordered mixing on turbulent skin friction, spiral longitudinal vortices were generated in a turbulent boundary layer. The boundary layer was formed on the test section wall of a facility designed especially for low-speed boundary layer studies. Screening tests which resulted in the choice and optimization of standard rectangular planform wall-mounted elements for producing this type of vortex are described. Skin friction and velocity profiles were measured as a function of longitudinal and transverse distance for several element configurations, and for the same flow condition. Element heights of 2, 10, and 20 percent of the boundary layer thickness were used. Effects on skin friction of the vortex-producing elements were measured up to 87 element heights downstream. Direct measurement of the element form drag was also made.

Author ↑

INTRODUCTION

The characteristics of the turbulent boundary layer have long posed a problem to those concerned with the efficiency of viscous flow. The relatively high values of skin friction drag and heat transfer rate associated with a turbulent boundary layer, compared to those for laminar flow, are well known. There has been considerable study into the feasibility of extending the range of laminar flow; that is, delaying the onset of turbulence. A certain degree of success has resulted from these studies, but in most practical cases the eventual transition to turbulent flow is inevitable. It would seem, therefore, that, in addition to developing techniques to retard the onset of turbulence, it is worthwhile to study the possibility of modifying the turbulent boundary layer in such a way as to reduce the undesirable effects.

The interest in using vortices to modify the turbulent boundary layer stems from somewhat fragmentary evidence (references 1, 2, 3) of their effects on a boundary layer. In at least one case (reference 3) a marked decrease in heat transfer resulted from the presence of the vortices implying a similar reduction in skin friction.

The choice of spiral longitudinal vortices in the subject investigation was due to their persistence, the desirability of extending any beneficial effects being obvious. In addition, a great deal of information on the production of this type of vortex in a shear layer is available. Finally, the

results; i.e., the effects of this common type of vortex-boundary layer interaction, would be of interest regardless of whether the effects are favorable.

This report presents the results of a set of experiments with spiral longitudinal vortices in a turbulent boundary layer. The efforts to optimize the experimental configuration are also described. The testing environment was created in the boundary layer facility of the LTV Research Center. Skin friction was measured directly, as well as mean velocity profiles, to determine the effects of the vortices. The results of these experiments were negative, in that no significant reduction in skin friction was measured; however, the experimental data, which are presented in sufficient detail to be useful, and the conclusions regarding the effects of the vortices should be of general interest.

SYMBOLS

AR	aspect ratio
C_f	local skin friction coefficient, τ_o/q
C_p	pressure coefficient, $p_o - p/q_{10}$ (where subscript 10 refers to X = 163.3 inches)
D	element drag
K	element height
p	static pressure
p_o	reservoir pressure
q	dynamic pressure, $\frac{1}{2} \rho U_\infty^2$
r_o	boundary layer channel radius
$R_{e\Theta}$	momentum thickness Reynolds number, $U_\infty \Theta/\nu$
U	local velocity
U_∞	free stream velocity
X	longitudinal distance measured from origin of laminar boundary layer
x	longitudinal distance downstream of element location
y	distance normal to wall
α	angle of attack
δ	boundary layer thickness

Θ boundary layer momentum thickness for axisymmetric flow, defined by:

$$r_o\Theta - \tfrac{1}{2}\Theta^2 = \int_o^{r_o} \frac{U}{U_\infty}\left(1 - \frac{U}{U_\infty}\right) r\, dr$$

ϕ azimuthal position

ω rotational speed in a vortex

ν kinematic viscosity

ρ density

τ_o wall shear stress

U_τ friction velocity, $\sqrt{\tau_o/q}$

Note: subscript sw refers to smooth wall conditions

INITIAL STUDIES

A. LITERATURE SEARCH

The spiral longitudinal vortex in a turbulent boundary layer has been dealt with by other experimenters on several occasions. The majority of this work has been devoted to the use of vortices as a mixing mechanism. The intent of the experiments has been to delay separation of boundary layer flow from its bounding surface in the presence of an adverse pressure gradient, such as exists in diffusers or on the aft portion of airfoil surfaces. The standard technique is the production of arrays of vortices near the edge of the boundary layer that mix the high energy fluid from the inviscid stream with the shear layer near the surface. This can be done with numerous types of vortex generators. The result is a net increase in energy near the surface which allows the flow to advance farther into an adverse pressure gradient before separation than is possible when the vortices are absent. Extensive experiments of this nature have been conducted at United Aircraft Corporation and the results can be found in references 4, 5, 6, and 7. The same type of work has also been done by the NACA and the National Bureau of Standards as reported in references 8, 9, and 10.

In most of these previous experiments the main objective has been to determine the controlling parameters and to optimize the mixing effects. Some of the important parameters have been found to be generator shape (i.e., lifting flat plates of various planforms, wedges, ramps, hemispheres, etc.) aspect ratio, generator height in the boundary layer, generator spacing, angle of attack to the flow (for lifting plates), and rotational sense of the vortices. In addition to studies of these parameters Schubauer and Spangenberg (reference 10) have investigated the effects on forced boundary layer mixing of

elements that were designed to mix the flow by deflection and displacement rather than through vortex action. A number of different mixing elements designed to have weak or non-existent trailing vortices were tested. In general these elements were of a wedge or plow-type shape. It was at first thought that intentional suppression of trailing vortices would reduce the momentum loss associated with the induced drag of the vortices. However, it was found that the body shapes necessary for vortex suppression had such an excessive surface area that the skin friction drag on the element itself nullified any gain realized by eliminating the induced drag of the vortices.

B. CHOICE OF PARAMETERS

In order to conduct a meaningful and systematic study of the vortex-boundary layer interaction phenomenon it was concluded that only a few of the many parameters should be varied at first and the effects of these variations analyzed. Then, based on these findings, the need for and the type of further experiments could be evaluated. The following paragraphs explain the process by which certain parameters were fixed.

1. Element Type

Considering all of the results found in references 1 through 10 it can be concluded that for forced boundary layer mixing the simple lifting flat plate element (plate in a plane normal to the surface) is an efficient device and is by far the simplest type to fabricate and use. Based on this conclusion the experiments described in this report were restricted to flat plate elements.

2. Planform

It would be desirable to have all of the vorticity created by an element concentrated into a single vortex which is released at the tip of the element. To accomplish this the circulation over the element span must be uniform and, for a non-uniform velocity field such as presented by a boundary layer, this can be achieved only by an appropriate choice of planform. In particular, the proper criterion is thought to be that the product of element chord and velocity, as a function of distance normal to the wall, should be held constant. Comparative tests (references 4 and 5) of elements tapered to match the velocity profile, rectangular elements, and trapezoidal elements (an approximation of the tapered case) have shown that the tip vortex strength, as implied by mixing efficiency, is indeed increased when the planform is tapered but the increase is small and from practical considerations the rectangular elements are the more desirable. Accordingly a rectangular planform was chosen for these experiments.

3. Element Height

The most important parameter would seem to be the height of the vortex-generating element as this determines the location of the vortex with respect to the bounding surface of the flow. The importance of this parameter lies in the fact that a shear flow will tend to dissipate any concentrated vortex motion. Thus, due to the velocity gradient in the boundary layer, the

distance of the vortex from the surface will, to some extent, affect its persistence in the flow. Also, little information is available in the literature concerning variations in this parameter, and it was obvious from the purpose of the reported experiments on the delay of separation that the optimum location for the vortices was at the edge of the boundary layer. For these reasons the element height was set as the primary variable.

4. Sense of Rotation

Elements may be inclined to the flow in such a way as to produce vortices that have the same rotational sense (co-rotating) or that will alternately have opposite rotational sense (counter-rotating). Both situations have been examined experimentally and analytically and compared for effectiveness (references 4, 5, and 7). Experiments and potential flow analyses have shown counter-rotating vortex arrays to be suprior mixers to co-rotating arrays. Potential flow analysis also shows that vortices in a counter-rotating array will tend to be attracted to or repelled from adjacent vortices in such a way as to group themselves in pairs due to interference effects caused by the induced velocity fields. However, experimental results show that this effect is actually very weak or non-existent. This is probably explainable by the fact that the true vortex motion damps out quickly downstream of the elements. The effects of the vortex, such as local three-dimensional distortion of the boundary layer, may persist quite a distance downstream, but the regions of distortion will not be moved laterally because of the quick dissipation of the induced velocity fields. Based on the above information the experiments reported herein have been restricted to counter-rotating vortex arrays.

5. Element Spacing

The choice of a spacing arrangement for the elements was somewhat arbitrary. The data in reference 7 show that mixing effectiveness is increased as the element spacing is decreased for equal spacing arrangements. Likewise the momentum deficit in the flow resulting from the form drag of the elements is increased due to the larger number of elements per transverse unit length. The velocity profiles show this effect in their change relative to the smooth wall profiles. The transversely averaged velocity near the wall is increased indicating stronger mixing action and implying higher skin friction for the closer spacings. Limited data for unequal spacings show that at spacing ratios as great as four to one (ratio of distance between elements lifting toward each other to distance between elements lifting away from each other) the velocity near the wall is significantly decreased in the decelerated regions and only slightly increased in the accelerated regions. This situation implies the condition of lowest transversely averaged velocity and hence lowest skin friction for all of the experiments described in reference 7. Therefore, for the experiments described herein, the element spacing parameter was fixed such that the distance between elements in a pair lifting away from each other was two element heights and the distance between elements of adjacent pairs was eight element heights, giving the four to one spacing ratio.

6. Aspect Ratio and Angle of Attack

The remaining parameters are element aspect ratio and angle of attack. Due to the strong influence of these parameters for an element of a

given height it was decided to conduct a series of screening tests to determine their optimum values. These tests along with the final detailed experiments are described in the following section.

EXPERIMENTAL PROGRAM

A. EXPERIMENTAL FACILITY

All of the experiments in this study were performed in the LTV Boundary Layer Channel. A complete description of this facility and its operating characteristics may be found in reference 11. By way of brief explanation the boundary layer channel is a straight circular tube having a test section 25 feet in length and eight inches internal diameter made up of six clear plexiglass sections. Operation is continuous and flow conditions are extremely steady. A vacuum blower, isolated from the test section by a sonic throat, pulls air at atmospheric pressure through a series of damping screens, a contraction section, and the test section. The flow may be investigated in detail at any location in the 25 foot test section. A sketch of the facility is shown in Figure 1.

The test environment for these experiments was a fully turbulent boundary layer created by artificial tripping of the laminar boundary layer near the entrance of the test section of the boundary layer channel. A constant mass flow rate was maintained during all testing. Figure 2 presents the rate of growth of the boundary layer, the free-stream velocity, and wall shear stress with distance down the channel for this mass flow rate. The abscissa in this figure is the distance in the downstream direction measured from the fictitious origin of the initially laminar boundary layer (see reference 11). The location of all elements tested in these experiments is also shown in this figure. Figure 3 is a photograph of a portion of the boundary layer channel showing the set-up for these experiments.

It has been pointed out in reference 11 that the boundary layer channel was designed for laminar boundary layer studies and for this case effectively produces a two-dimensional flow field. However, it will be noticed that the turbulent boundary layer thickness, shown in Figure 2, is not small with respect to the channel radius and thus cannot be treated two-dimensionally. In addition, the free stream conditions change according to the boundary layer growth. The conditions are such that the nature of this particular flow places it in the regime of pipe entrance flow rather than simple boundary layer flow such as exists on a flat plate. Consequently any analysis of the flow must take into account the longitudinal pressure gradient and three-dimensional effects. This will be covered in more detail in the following sections.

The boundary layer channel is instrumented with conventional flow measuring apparatus such as total pressure probes, static pressure wall ports, static pressure probes, and hot-wire anemometer probes. In addition a special, and somewhat unique, skin friction balance has been built for the channel that allows very accurate measurements of local skin friction drag to be made. This balance has been reported in detail in reference 12 and was used extensively in these experiments. For these experiments all velocity profiles were measured with a small total pressure probe having an opening 0.003 inches high by 0.040

inches wide, used in conjunction with a differential capacitance transducer (Equibar Pressure Meter, manufactured by Transonics, Inc.).

B. SCREENING TESTS

As mentioned previously the variable parameters for the experiments were reduced to three (element height, angle of attack, and aspect ratio) from conclusions based on information in the literature. It was desired to further narrow the number of variables to a single parameter which was picked as the element height. In an attempt to determine the optimum values for aspect ratio and angle of attack a series of screening tests were run with measurements being made of the relative vortex strengths and the element form drag as these parameters were varied. This was accomplished by measuring the vortex strength with a rotating-vane vorticity meter and measuring the element form drag by attaching the elements directly to the surface of the skin friction balance disk. The ratio of rotational speed in the vortex to the drag of the element was taken as the significant parameter for determining the optimum values of aspect ratio and angle of attack for the vortex-generating elements.

Several different elements were tried. Rectangular elements of height 0.81 inches with aspect ratios of 1.3, 1.5, and 2.0; height of 0.31 inches with aspect ratios of 1.3 and 1.5; and height of 0.50 inches with aspect ratio of 1.5 were tested. For comparison, some measurements were also made with a trapezoidal element 0.31 inches in height with an aspect ratio of 0.65 and a 0.50-inch high element with an aspect ratio of 1.5 tapered to match a 1/7-power turbulent boundary layer profile.

The results of these tests are shown in Figure 4. Rotational speeds in the vortices at a distance 18 inches downstream of the elements were determined by measuring the speed of the vorticity meter with a stroboscope. Even though the vorticity meter was mounted in jeweled instrument bearings the slight friction was enough to prevent measurements being made for the smaller elements at the lower angles of attack. The measured form drag, rotational speed, and the ratio of rotational speed to form drag are shown. The data for the larger elements show that a maximum of this ratio occurs near an angle of attack of eight degrees; in addition, the rotational speed itself approaches a constant value near eight degrees. The data for the smaller elements are insufficient to show this but do indicate the same trends as the larger elements beyond eight degrees.

Some visual studies were also made by introducing a streamer of smoke into the flow near the wall so that the elements were immersed in it. In this way it was possible to see the shed vortices. These tests confirmed the fact that there is little difference in the performance of rectangular and tapered planform elements. An interesting observation was made when the elements were set such that a very slight clearance existed between them and the wall. A very complicated pattern of multiple vortices would appear at the wall which seemed to depend strongly on the amount of clearance and the angle of attack of the elements.

As pointed out previously these screening tests were only for comparative purposes and, with the possible exceptions of the drag measurements

and optimum angle of attack the data should not be taken as absolute. The results were sufficient to allow a reasonable choice of angle of attack and aspect ratio to be made. These were picked as eight degrees and 1.3 respectively.

C. FINAL EXPERIMENTS

The final experiments were performed with three sizes of elements. Rectangular elements measuring 0.500 inches by 0.770 inches, 0.250 inches by 0.385 inches, and 0.050 inches by 0.077 inches were mounted on the wall at a fixed longitudinal station and spaced continuously around the inside circumference of the boundary layer channel. In each case the aspect ratio was 1.3 and the angles of attack were fixed at plus and minus eight degrees. The spacings for each array were two element heights between elements in a pair lifting away from each other and eight element heights between elements of adjacent pairs. The geometry of an elemental array is shown in Figure 5 expressed in terms of element height, K. This geometry was similar for each of the three arrays.

The first test for each element size was the effect on longitudinal pressure gradient in the flow. As mentioned previously the inviscid flow environment was dependent on the boundary layer; therefore, it was necessary to determine the effects of the elements on the boundary layer flow.

In the course of the work reported in reference 12 it was found that the measured values of skin friction coefficient in the undisturbed turbulent flow were less than those for either flat-plate boundary layers or fully developed pipe flow at the same Reynolds number. The skin friction coefficient was also found to be dependent upon the ratio of boundary layer momentum thickness to channel radius. A relation was found which satisfactorily correlated the smooth-wall data. In this correlation the skin friction coefficient was found to be expressed as $C_f = C_f (R_{e\Theta}, \Theta/r_o)$ where r_o is the boundary layer channel radius and Θ is momentum thickness defined for axisymmetric flow. It is obvious from this correlation that the interdependence of pressure gradient, boundary layer growth, and three-dimensional effects is important in determining the skin friction.

It was desirable to be able to directly compare skin friction measurements made with and without the elements present. To do this the free stream flow conditions (longitudinal pressure gradient and velocity distribution) must remain unchanged for both configurations to avoid the introduction of extraneous three-dimensional effects that would affect the skin friction. Otherwise a comparison of the skin friction would involve a more complicated analysis.

In order to determine whether or not this problem existed static pressure measurements were made in the channel for each array of elements. The longitudinal static pressure gradient was determined from measurements at the wall and comparisons were made with static pressures determined with a probe at various locations in the stream at the same longitudinal station. No measurable differences in static pressure were found in either the direction normal to the wall or in the azimuthal direction.

The longitudinal pressure gradient data are shown in Figure 6. The

solid curve in this figure represents the pressure gradient for the flow with no elements present. The data for all sizes of elements are plotted for comparison with this curve. The data are presented non-dimensionally as the local static pressure drop referenced to the entrance section of the boundary layer channel divided by the free stream dynamic pressure at a station ($X = 163.3$ inches) just upstream from the element location. The data show that no significant effect in longitudinal pressure gradient exists. This implies that no measurable net effect results, although the boundary layer is locally thickened or thinned by the action of the elements and vortices. Consequently, free stream flow conditions are the same with and without the elements as is also shown in Figure 6, and skin friction measurements can be compared directly.

The next step in the experimental program was a check of the symmetry in the flow. Velocity profiles were measured at five azimuthal positions covering one cycle of the element array. In all cases the symmetry was found to be good, and for the final experiments profiles were measured only over one half-cycle of an element array in order to conserve time.

The final step was the detailed measurement of velocity profiles and skin friction drag for each array of elements. Velocity profiles were measured at three azimuthal positions at each longitudinal station downstream of the elements. These azimuthal positions are defined in Figure 5 as ϕ_1, ϕ_2, ϕ_3. The velocity profiles are shown in Figures 7 through 11 compared to the appropriate profiles for the flow with no elements. Figure 12 presents velocity profiles for the 0.50-inch elements in the form of the universal law of the wall parameters compared to Coles' (reference 13) curve determined empirically for incompressible turbulent flow over a flat plate.

The skin friction data are shown in Figures 13 through 18 compared to the skin friction on the wall of the channel with no elements. The variation in wall shear stress with longitudinal and azimuthal positions are shown as well as the longitudinal variation of the azimuthally integrated average shear stress.

Interpretation and discussion of these results are covered in the next section.

DISCUSSION OF RESULTS

Figures 7 through 15 give the velocity profiles and skin friction measurements for the primary element configurations tested - fixed angle of attack, aspect ratio, and spacing; and three element heights. It is well to note the organization of these figures as they show the effect of the vortices on the velocity profile - and the attendant effect on the skin friction - as a function of both longitudinal and azimuthal position.

Figures 7 and 10 show the same velocity profile data for 0.50 - inch elements with both longitudinal and azimuthal position, respectively, as independent variables. The data are compared with the smooth wall velocity profiles in both cases. In Figure 10 the distance from the wall is made

dimensionless by dividing by the appropriate smooth wall boundary layer thickness, δ_{sw}, taken from Figure 2. Figure 13 gives the local shear stress as a function of azimuthal position for the three different longitudinal stations corresponding to the velocity profiles. The shear stress is normalized with respect to the corresponding shear stress for the smooth wall taken from Figure 2. Both the velocity profiles and the skin friction measurements show locally strong transverse variations. These transverse variations damp more quickly with longitudinal distance directly behind an element pair than between pairs (see Figure 10). In addition, where the local velocity near the wall is lower than that of the smooth wall the local shear stress is also lower. In these figures, the boundary layer is not thickened measurably, and the effects on the velocity profile and skin friction persist at least 81.6 element heights downstream.

Figures 8 and 11 show the velocity profiles and Figure 14 shows the local shear stress for the 0.25 - inch elements. These data show the same general pattern as seen for the 0.50-inch elements, although diminished in strength. The effect is seen to persist at least 67.2 element heights downstream. Note the difference in shape of the curves for azimuthal variation of shear stress for the 0.50 and 0.25-inch elements. Part of this difference in shape is due to the size of the two systems of vortices relative to the balance disk size and planform. The balance disk averages the local effects differently for the two systems; i.e., the data for the larger elements represent the local effects more accuratly than do the data for the smaller elements.

Figures 9 and 15 give the velocity profiles and skin friction, respectively, for the 0.05-inch elements. Since very little effect was noted at the positions shown, no further tests were made with these elements. The data prompt the question of whether there were vortices generated by these small elements, or whether the effects of the vortices generated were simply insignificant. Since flow visualization with these small elements was not possible, the question remains unanswered.

Figure 12 presents the velocity profiles for the 0.50-inch elements in law of the wall parameters. Comparison of turbulent velocity profile data with the accepted incompressible correlation of Coles is one way of determining the residual effects of disturbances introduced into the turbulent boundary layer. This relation emphasizes the profile near the wall, whereas the velocity defect relation emphasizes the flow in the outer part of the profile. Both types include the wall shear stress as a part of the correlation. The disturbed turbulent boundary layer profile can be thought to approach a shape given by both correlations as the disturbances dissipate. Figure 12 shows that the data deviate from the law of the wall correlation at large values of yu_τ/ν - as already seen in Figures 7 through 11 - although the data near the wall agree well with the correlation. This points out that this correlation applies near the wall for a boundary layer disturbed in this manner - even for profiles very near the elements. The law of the wall profiles for the other elements exhibit the same trends.

Figure 16 is a compilation of the shear stress data from the previous figures. The azimuthally integrated average shear stress normalized with respect to smooth wall shear stress, is shown as a function of x/K for the three element heights. Except for measurements very near the elements the average shear stress is increased. The values of average shear stress appear to reach a maximum and approach an asymptote for large x/K.

The net increase in skin friction can be shown to be due primarily to the added mixing, with no appreciable effect added by the form drag of the elements. The remarks in the section about the experimental facility indicated that if the momentum thickness is changed by the momentum losses of the elements (independent of the change in momentum thickness Reynolds number) the shear stress will change accordingly. Direct measurement of element form drag, which is listed in Figure 16, allowed the calculation of the increase in momentum thickness due to form drag. For the 0.50-inch elements, this amounts to a three percent change in momentum thickness, which causes an insignificant change in shear stress. This fact, coupled with the unchanged free stream conditions, made it possible to directly determine the effects of the vortices on the skin friction.

Figures 17 and 18 show the effects of changes in element spacing for the 0.25-inch elements (keeping the aspect ratio, angle of attack and longitudinal station constant). The configuration in Figure 17 amounts to reversing the rotation of the vortices from that of the previous experiments. The azimuthal pattern of shear stress variation is seen to change phase by one-half cycle for the rotation reversal. This indicates little interaction of the vortices with each other for this configuration. The normalized azimuthally integrated average shear stress is 1.02 for the reversed rotation, as compared with 1.02 for the previous case.

Figure 18 shows the shear stress variation for approximately equal spacing of elements. The integrated average shear stress is 1.02, again showing little mutual interaction of vortices. The implication is that the net effect on skin friction depends only on the number of elements per unit transverse length and not on the relative spacing. This behavior may not be generally true but the results shown here indicate that further studies in this area might be beneficial to those interested in vortex generators as mixing devices.

In regard to the mutual interaction of vortices, the direct measurement of form drag also showed no interaction effects for elements spaced from two to an infinite number of element heights apart.

CONCLUSIONS

Analysis of the experimental data resulted in the following conclusions:

1. For the configurations tested, designed to produce strong mixing in the boundary layer, the skin friction is both decreased and increased locally, but the integrated effect, greater than a few element heights downstream, is to increase the skin friction.

2. The major effect on skin friction is found to be due to the mixing added by the vortices, whereas the effect of the form drag of the elements is not significant.

3. Vortices generated well inside the turbulent boundary layer affect the skin friction and velocity profile far downstream of the point of origination.

4. There is an indication from the limited data taken with the different spacing arrangements that the average effect on skin friction depends only on the number of elements per unit transverse length and not on the spacing. This implies that the mutual interference effects of the vortices are small for the spacings tested.

5. For the configurations tested, the ratio of angular velocity to form drag is a maximum, and the angular velocity approaches a constant value, near an element angle of attack of eight degrees. Therefore, an unnecessary form drag penalty is incurred by operation of this type of element at greater angles of attack, regardless of the application of the increased mixing.

ACKNOWLEDGEMENTS

The work described in this report has been done in the LTV Research Center Aerophysics Group under the supervision of Dr. John Harkness. The authors wish to express their appreciation to Dr. Harkness, Dr. F. W. Fenter, and Mr. W. A. Meyer for their interest in and assistance with this program, and to Mr. C. H. Parker for his valuable assistance in fabrication and operation of the experimental apparatus. This program is supported by independent research and development funds of Ling-Temco-Vought, Inc. Additional support was provided during 1963-64 by the National Aeronautics and Space Administration under Contract No. NASw-730. This support is being continued during 1964-65 under contract No. NASw-956.

REFERENCES

1. Eggers, A. J., Jr., and Hermach, C. A., "Initial Experiments on the Aerodynamic Cooling Associated with Large-Scale Vortical Motions in Supersonic Flow", NACA RM A54L13, 1955.

2. Van Driest, E. R., and McCauley, W. D., "The Effect of Controlled Three-Dimensional Roughness on Boundary Layer Transition at Supersonic Speeds", J.A.S., April, 1960.

3. Kline, S. J., and Runstadler, P. W., "Some Preliminary Results of Visual Studies of the Flow Model of the Wall Layers of the Turbulent Boundary Layer", Trans. of the ASME, June, 1959.

4. Taylor, H. D., "The Elimination of Diffuser Separation by Vortex Generators", United Aircraft Corp. Report R-4012-3, June 10, 1947.

5. Taylor, H. D., "Application of Vortex Generator Mixing Principle to Diffusers", United Aircraft Corp. Report R-15064-5, December 31, 1948.

6. Powers, W. E., "Application of Vortex Generators for Boundary Layer Control Through a Shock", United Aircraft Corp. Report R-95477-6, July 11, 1952.

7. Grose, R. M., "Theoretical and Experimental Investigation of Various Types of Vortex Generators", United Aircraft Corp. Report R-15362-5, March 16, 1954.

8. McCullough, G. B., Nitzberg, G. E., and Kelly, J. A., "Preliminary Investigation of the Delay of Turbulent Flow Separation by Means of Wedge-Shaped Bodies", NACA RM A50L12, March 1, 1951.

9. Weiberg, J. A. and McCullough, G. B., "Wind-Tunnel Investigation at Low Speed of a Twisted and Cambered Wing Swept Back 63° with Vortex Generators and Fences", NACA RM A52A17, March 25, 1952.

10. Schubauer, G. B., and Spangenberg, W. B., "Forced Mixing in Boundary Layers", National Bureau of Standards Report 6107, August 8, 1958.

11. Wells, C. S., Jr., and Spangler, J. G., "A Facility for Basic Boundary Layer Experiments", LTV Research Center Report No. 0-71000/2R-32, November 1962.

12. Spangler, J. G., "A Sensitive Magnetic Balance for the Direct Measurement of Skin Friction Drag", LTV Research Center Report No. 0-71000/3R-29, December 1963.

13. Coles, D., "Measurements in the Boundary Layer on a Smooth Flat Plate in Supersonic Flow", Ph.D. Thesis, California Institute of Technology, 1953.

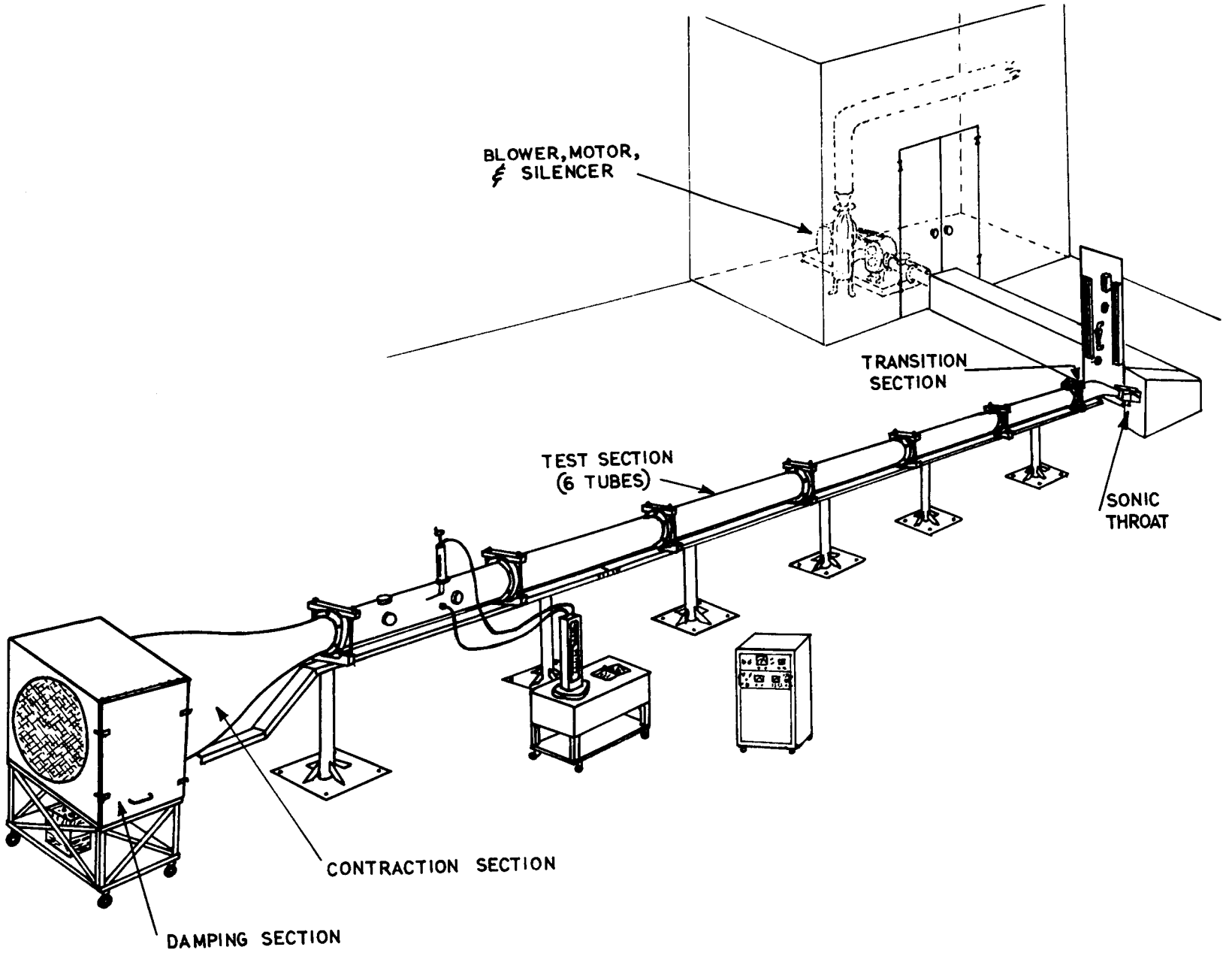

Figure 1 A portion of the Aerophysics Laboratory showing the boundary layer channel.

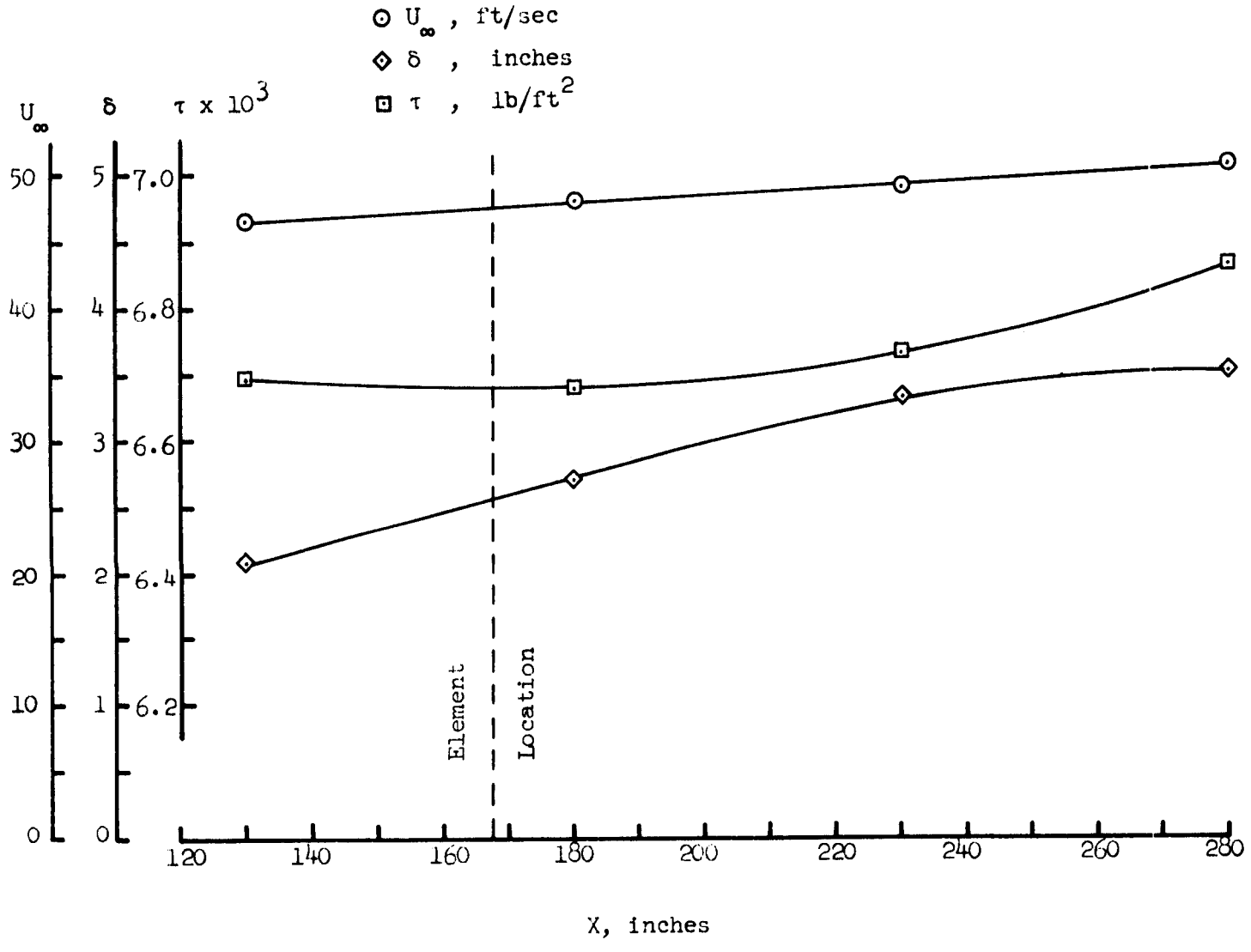

Figure 2 Variation of free stream velocity, boundary layer thickness and wall shear stress with longitudinal position for smooth wall configuration.

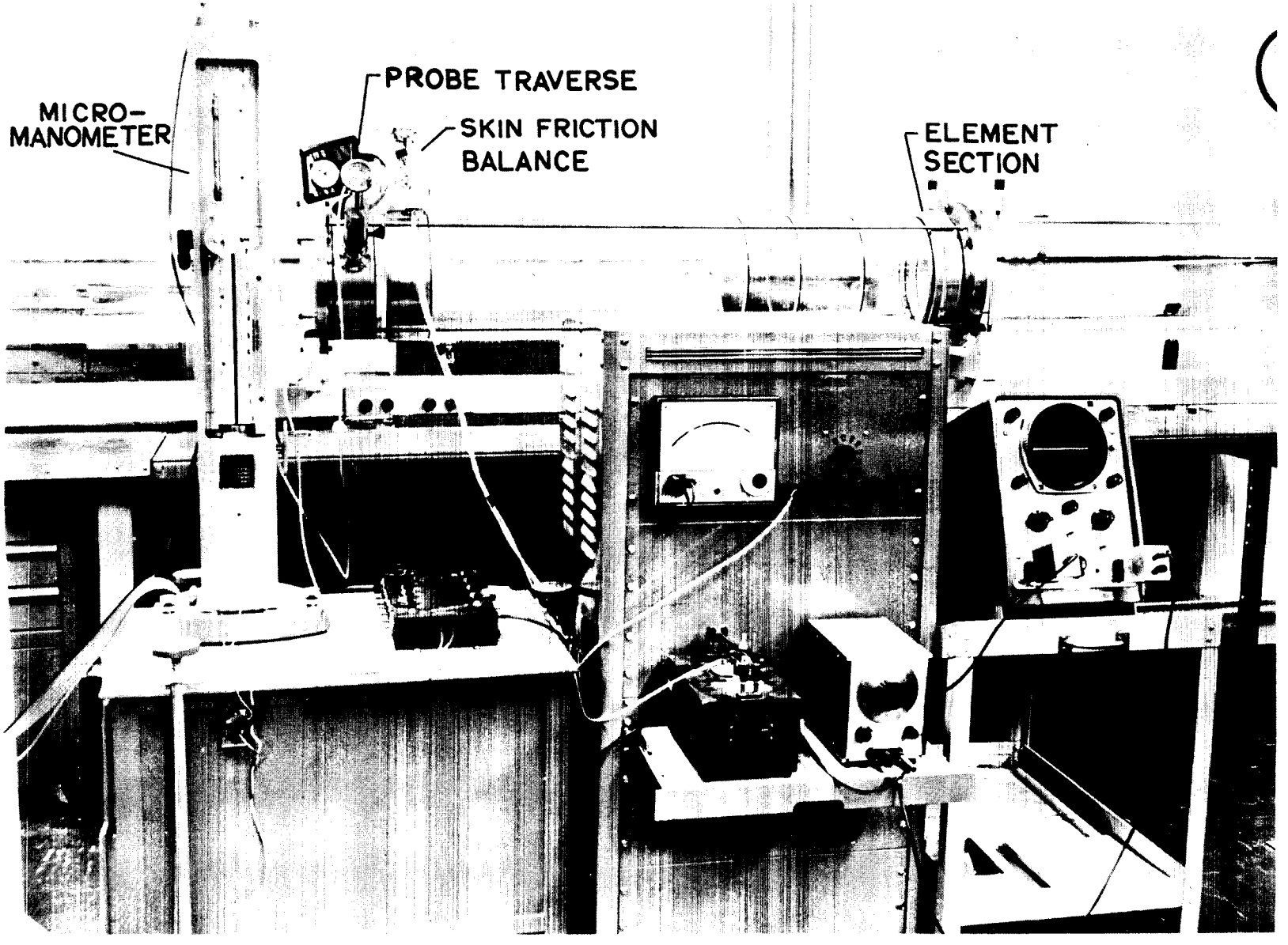

Figure 3 A portion of the experimental set-up.

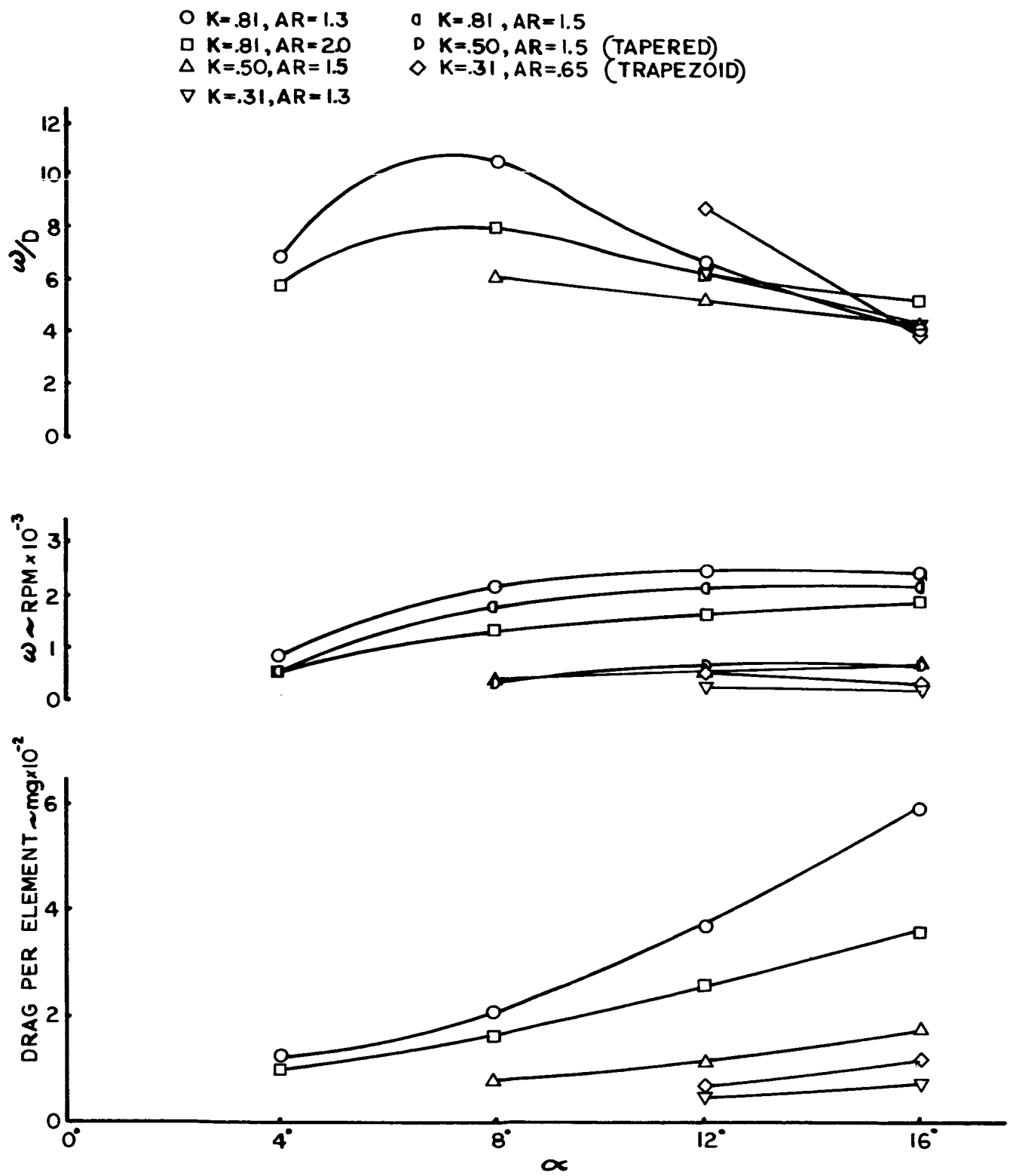

Figure 4 Results of screening tests.

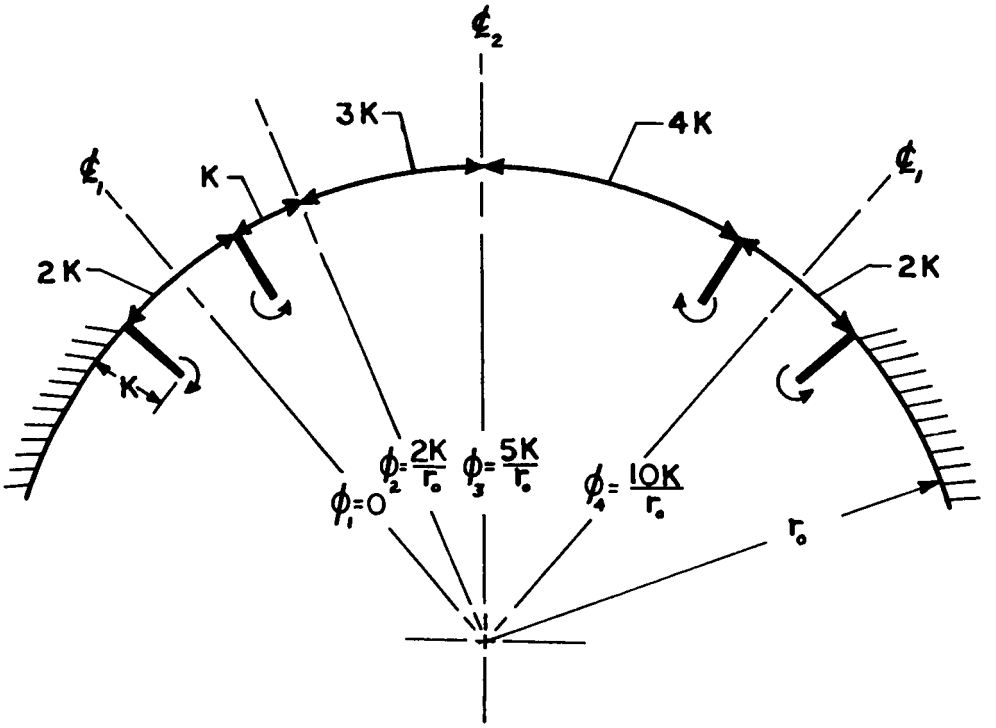

$\mathcal{L}_1$ = Centerline of Element Pair

$\mathcal{L}_2$ = Centerline of Adjacent Pairs

K = Element Height

r_o = Boundary Layer Channel Radius

ϕ = Azimuthal Location Measured from $\mathcal{L}$ of an Element Pair

Figure 5 Geometry of an elemental array.

EFFECTS OF SPIRAL LONGITUDINAL VORTICES ON TURBULENT BOUNDARY LAYER SKIN FRICTION

By J. G. Spangler and C. S. Wells, Jr.

Prepared under Contract No. NASw-956 by
LING-TEMCO-VOUGHT, INC.
Dallas, Texas

for

NATIONAL AERONAUTICS AND SPACE ADMINISTRATION

For sale by the Office of Technical Services, Department of Commerce,
Washington, D.C. 20230 -- Price $2.00

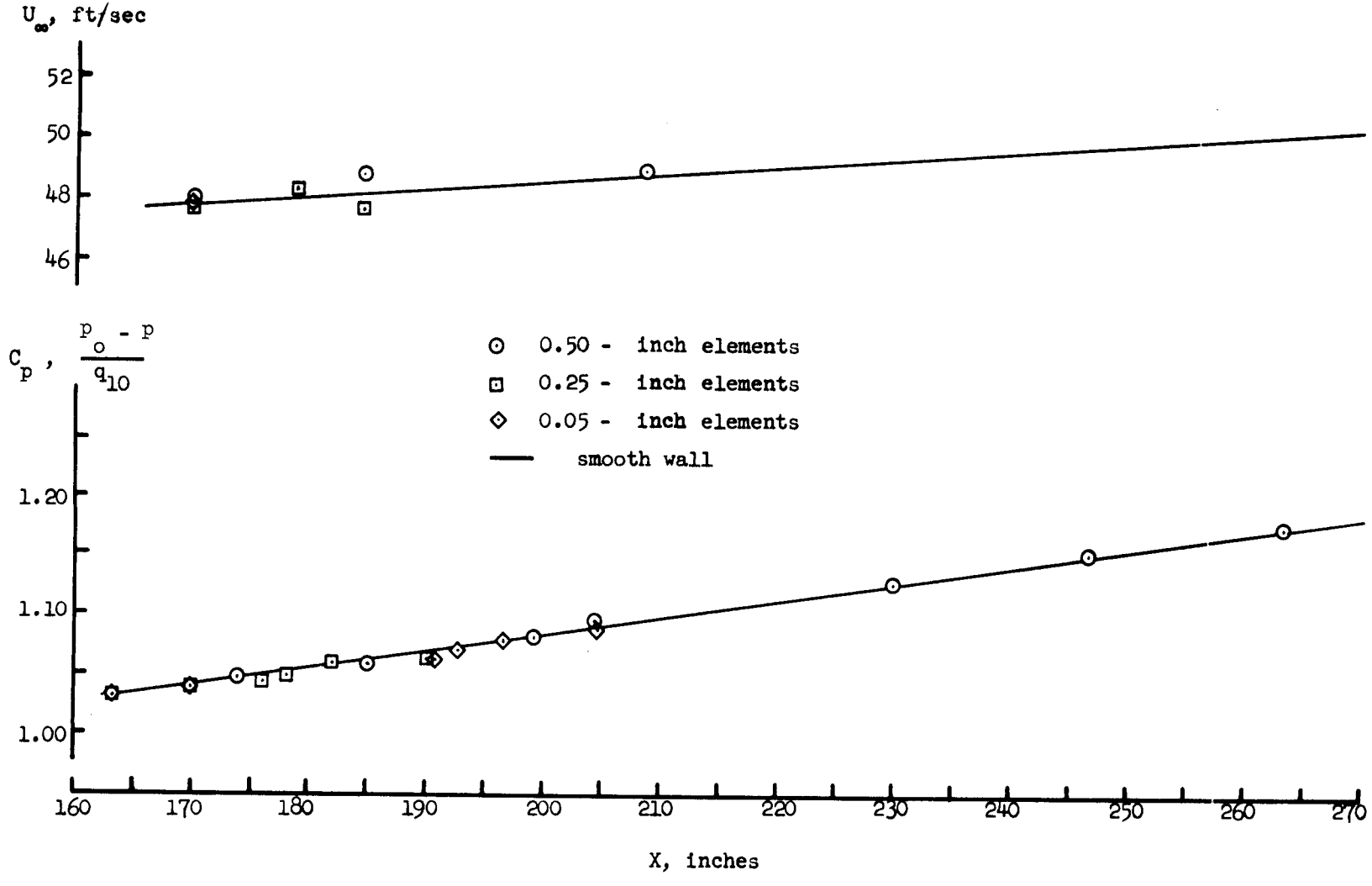

Figure 6 Longitudinal variation of static pressure and free stream velocity.

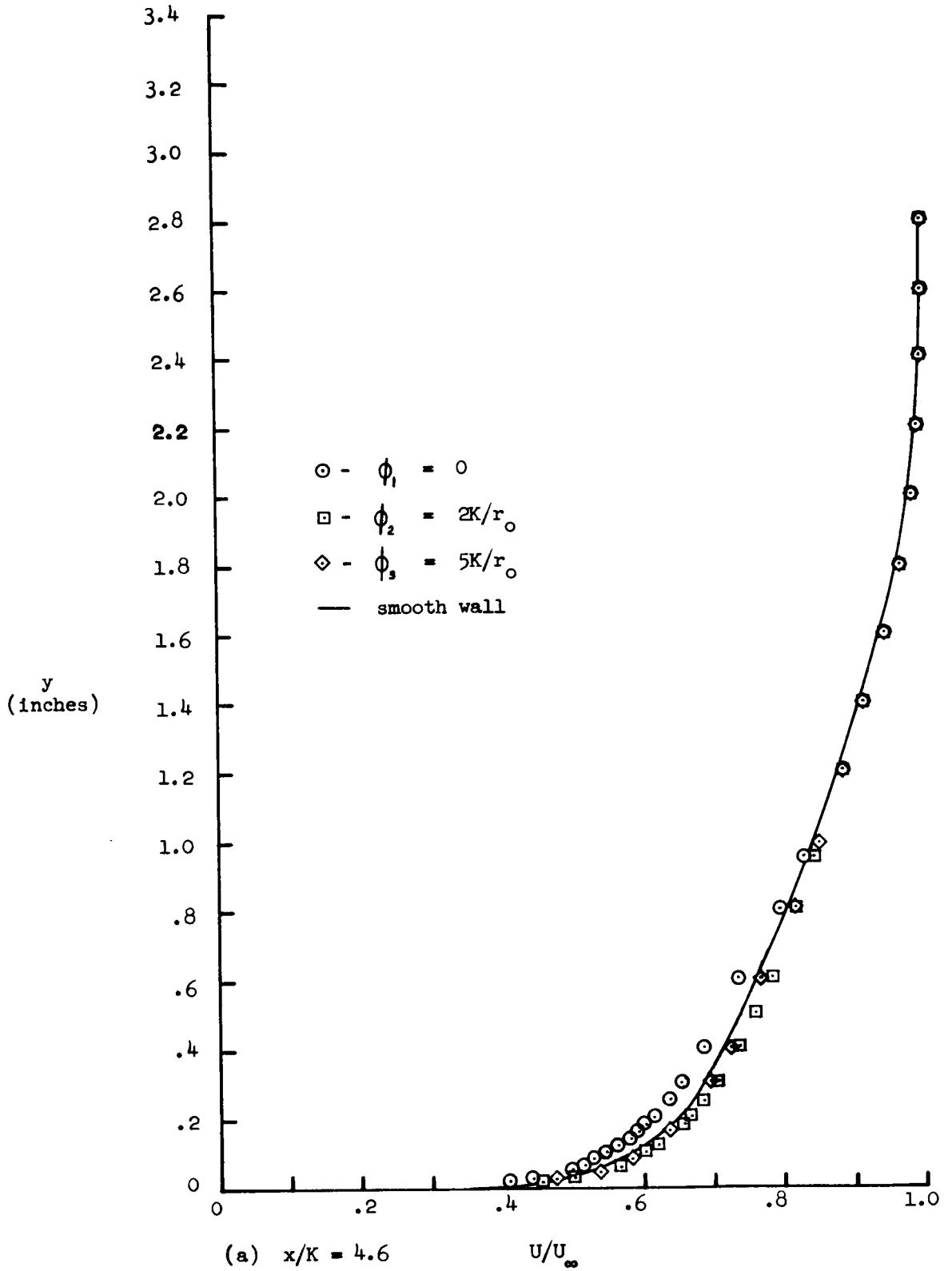

Figure 7 Azimuthal variation of boundary layer velocity profiles downstream of 0.50 - inch elements.

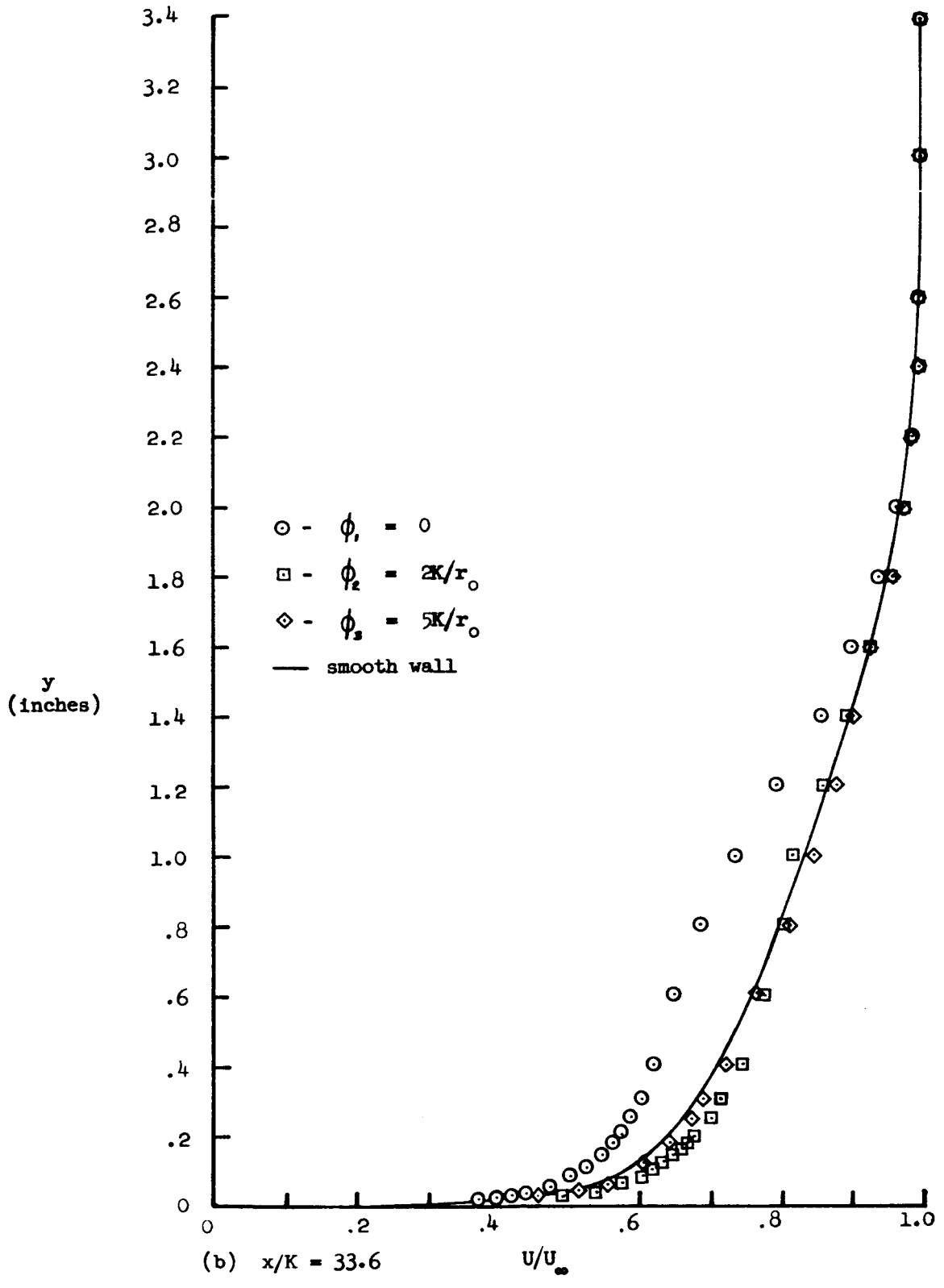

Figure 7 (Continued) Azimuthal variation of boundary layer velocity profiles downstream of 0.50 - inch elements.

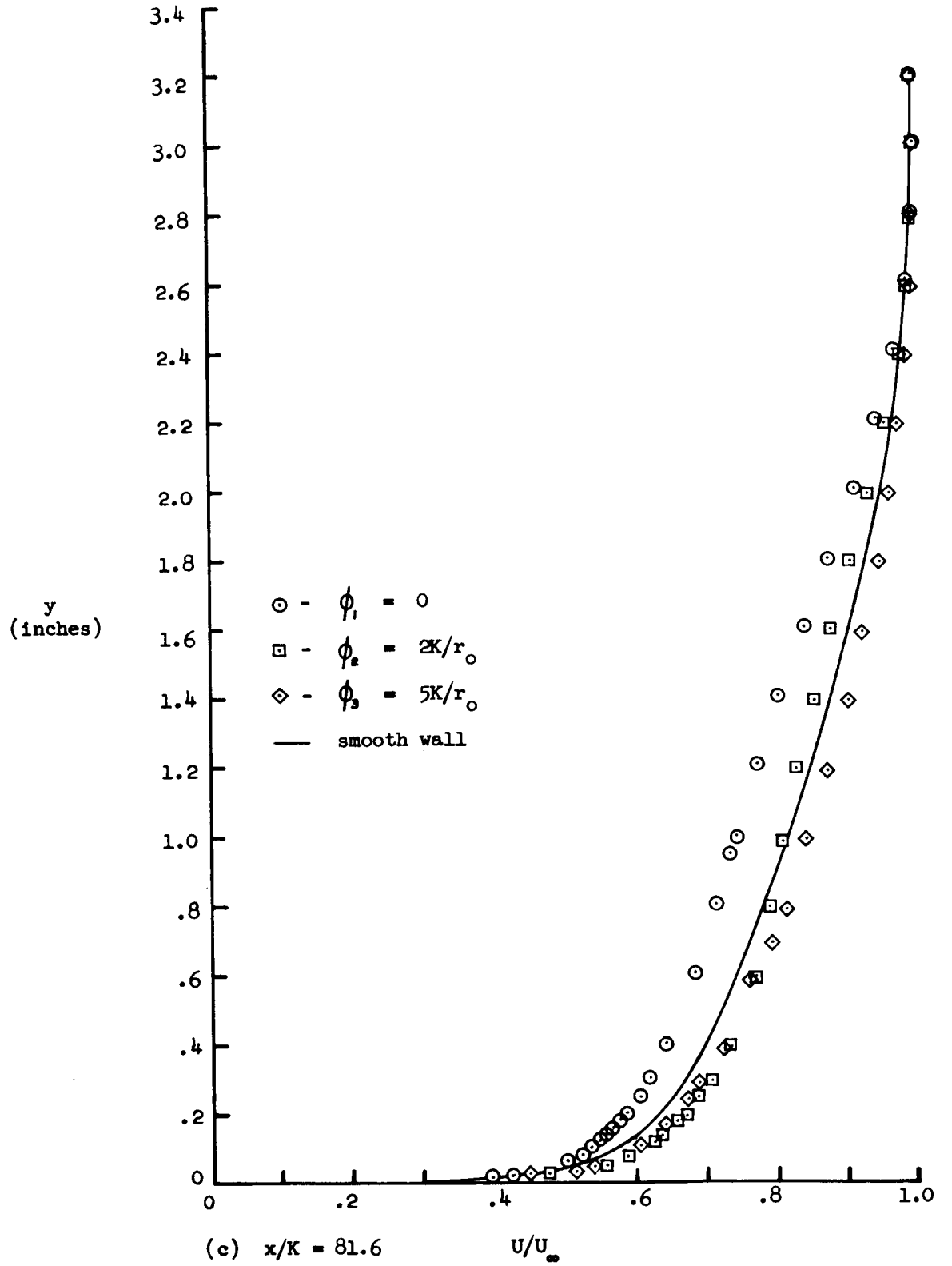

Figure 7 (Concluded) Azimuthal variation of boundary layer velocity profiles downstream of 0.50 - inch elements.

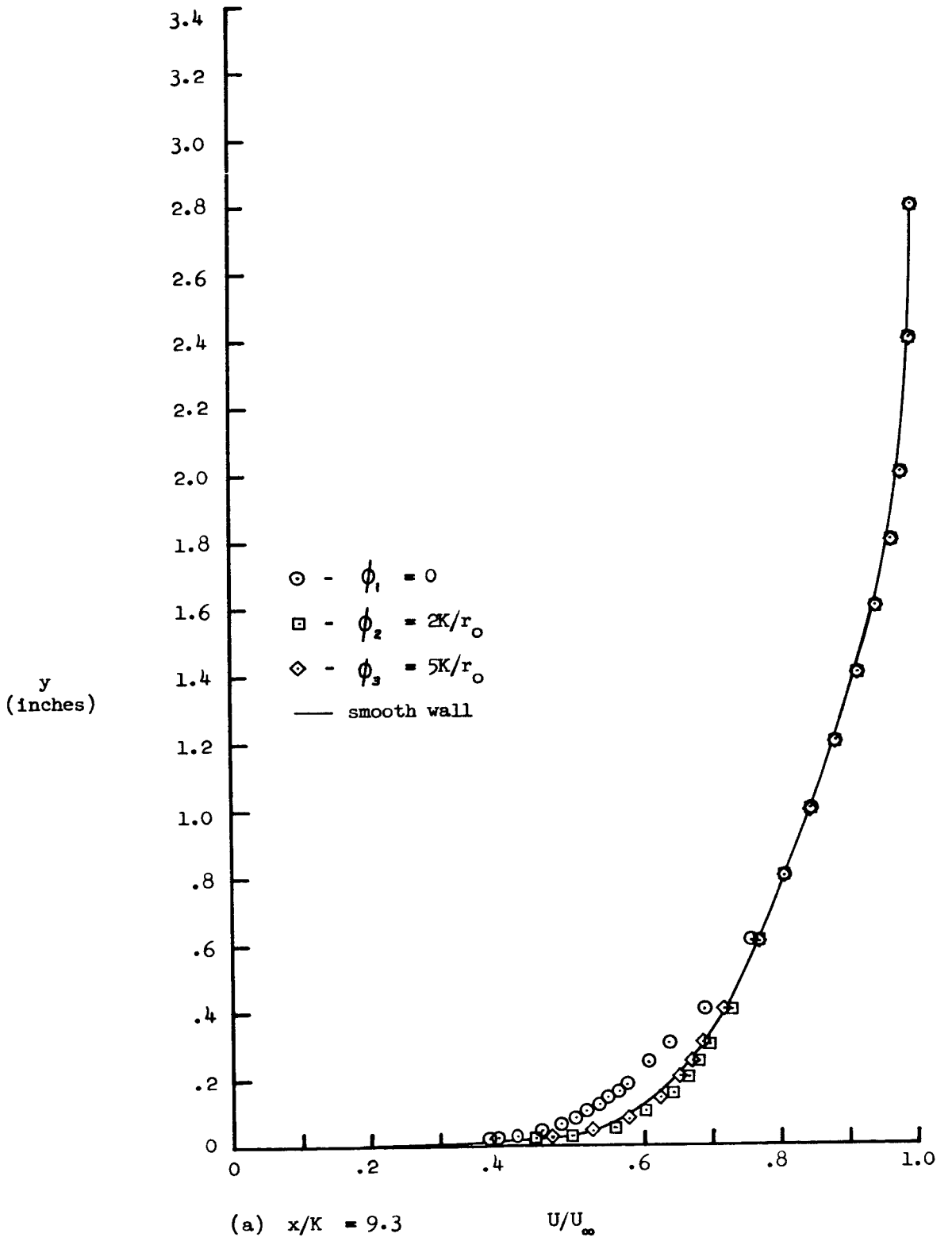

Figure 8 Azimuthal variation of boundary layer velocity profiles downstream of 0.25 - inch elements.

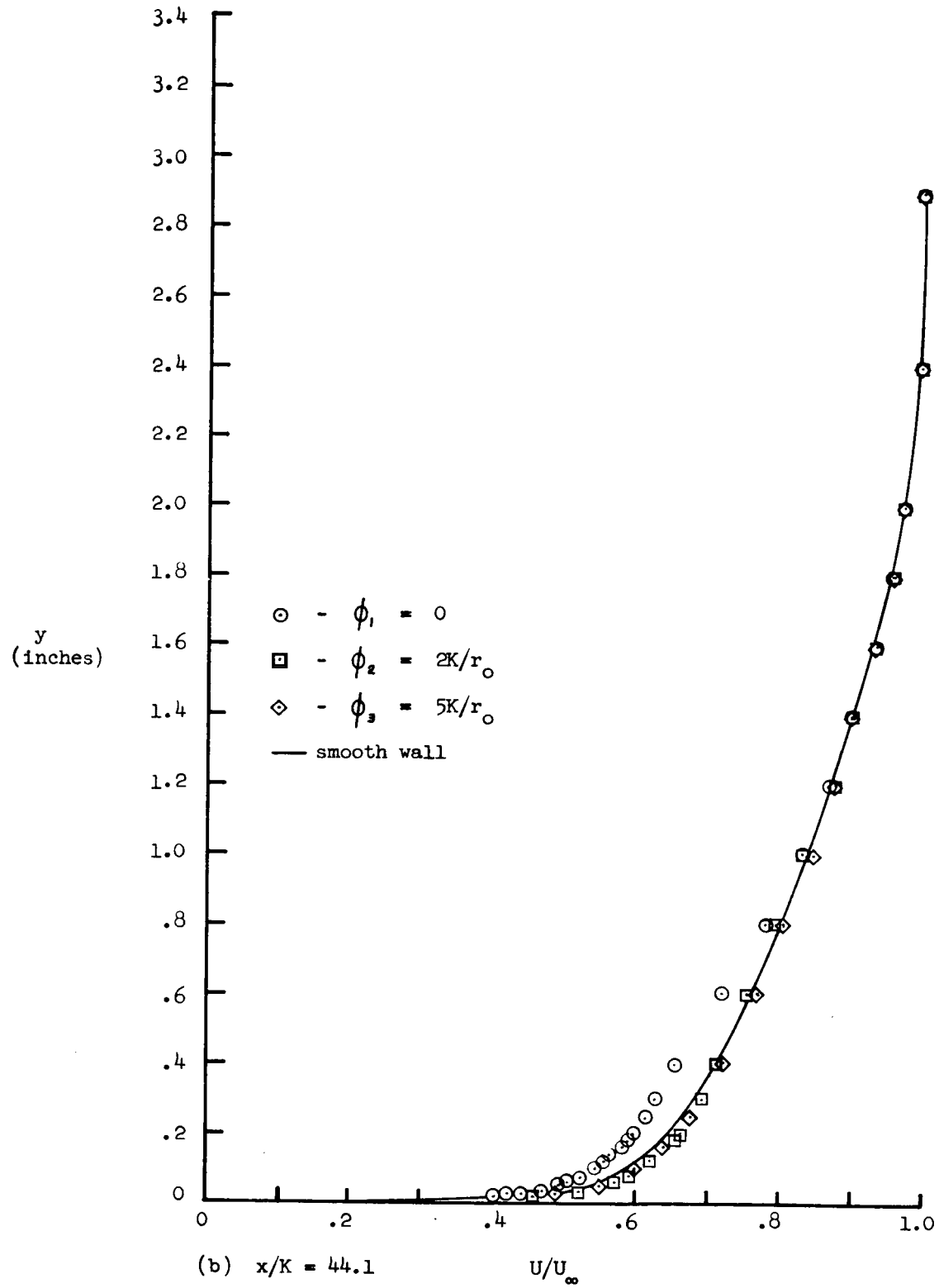

Figure 8 (Continued) Azimuthal variation of boundary layer velocity profiles downstream of 0.25 - inch elements.

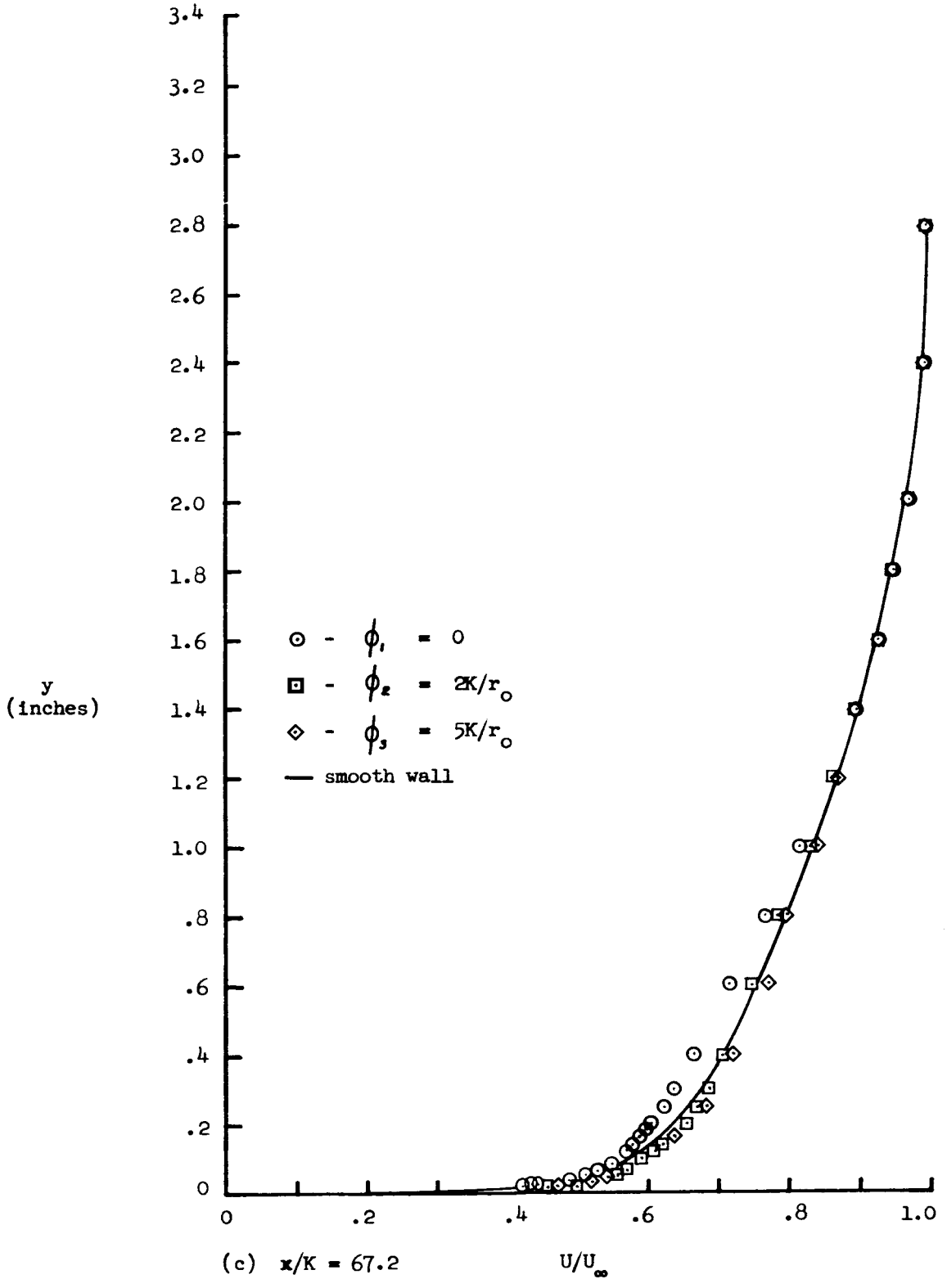

Figure 8 (Concluded) Azimuthal variation of boundary layer velocity profiles downstream of 0.25 - inch elements.

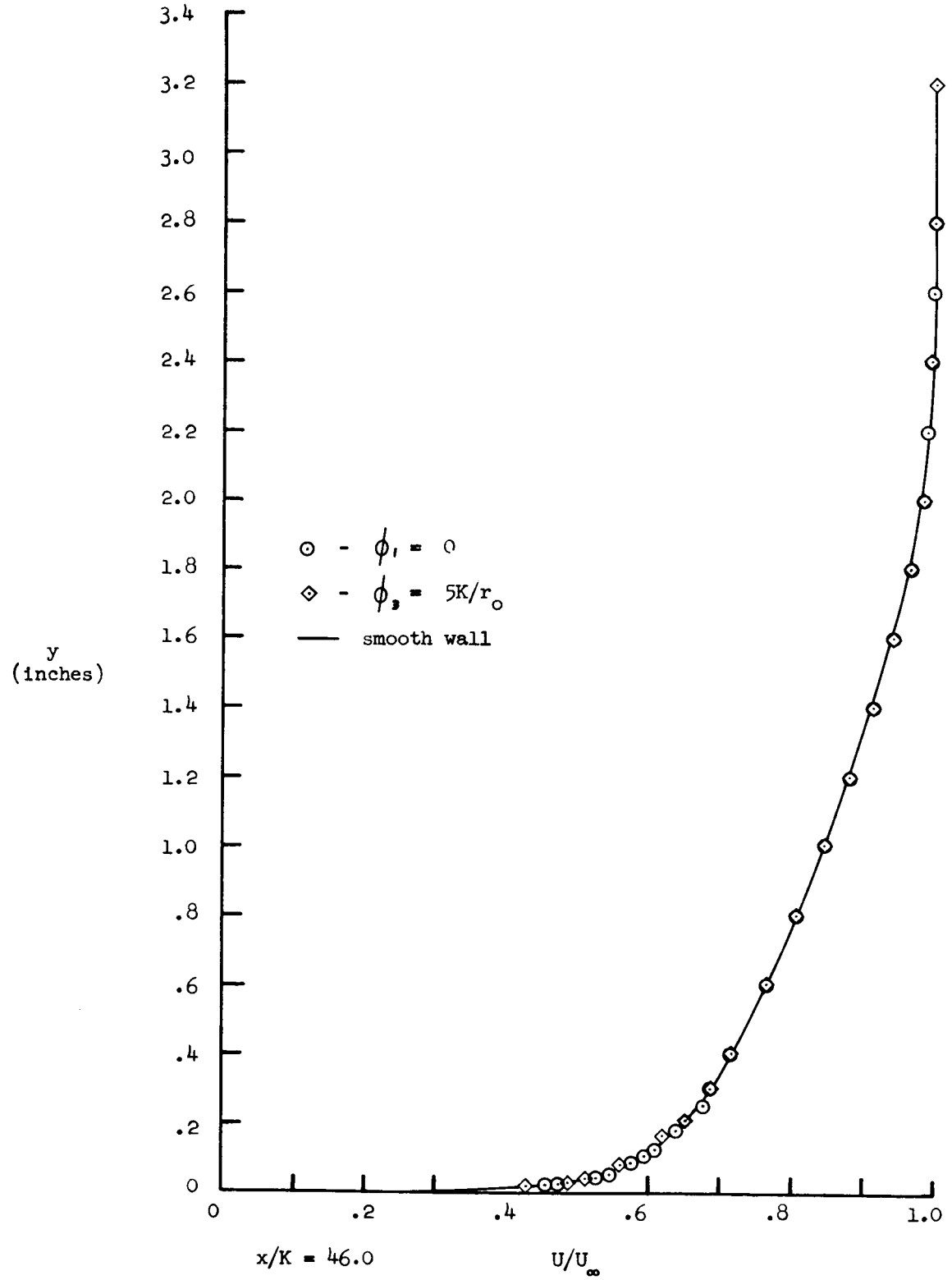

Figure 9 Azimuthal variation of boundary layer velocity profiles downstream of 0.05 - inch elements.

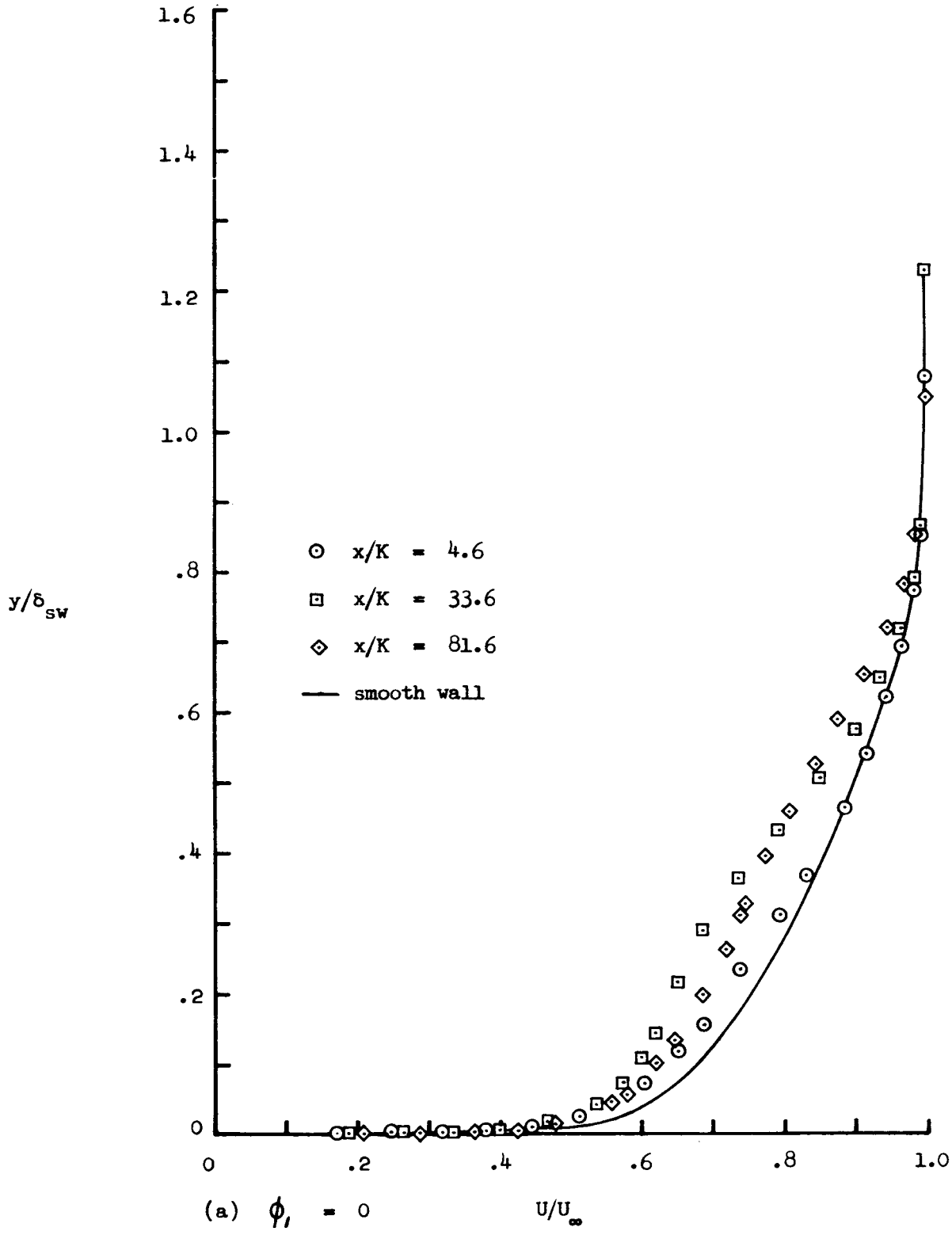

Figure 10 Longitudinal variation of boundary layer velocity profiles downstream of 0.50 - inch elements.

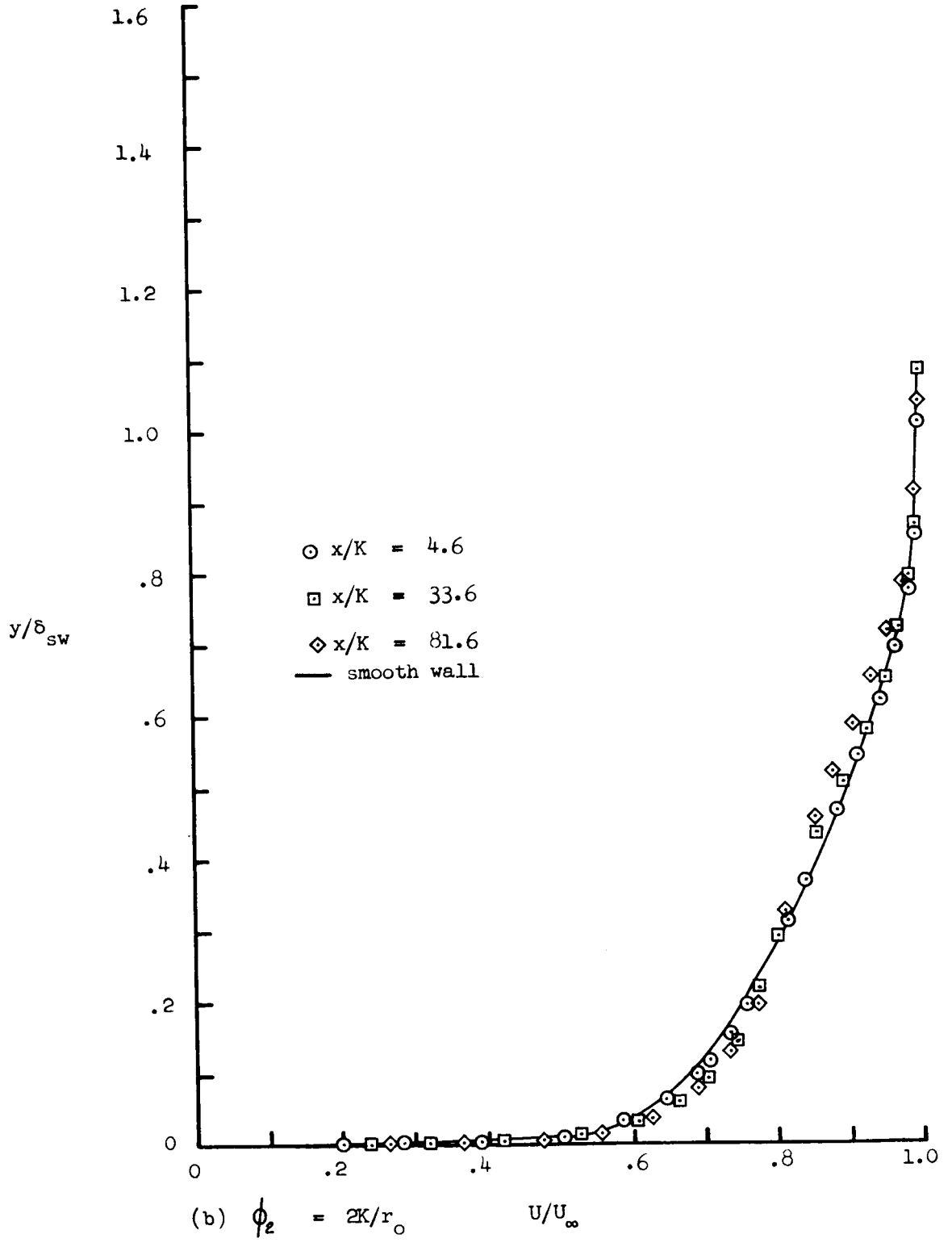

Figure 10 (Continued) Longitudinal variation of boundary layer velocity profiles downstream of 0.50 - inch elements.

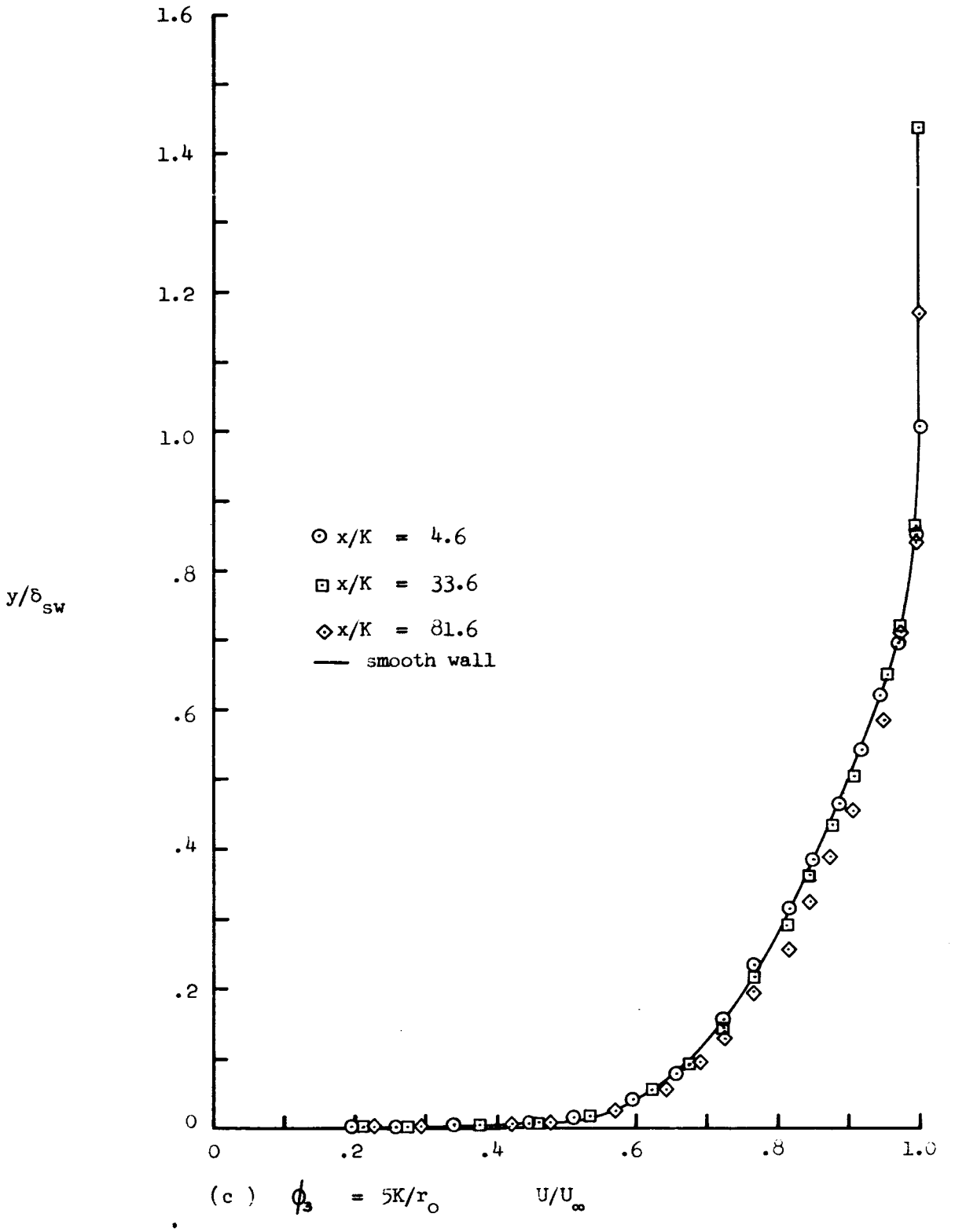

Figure 10 (Concluded) Longitudinal variation of boundary layer velocity profiles downstream of 0.50 - inch elements.

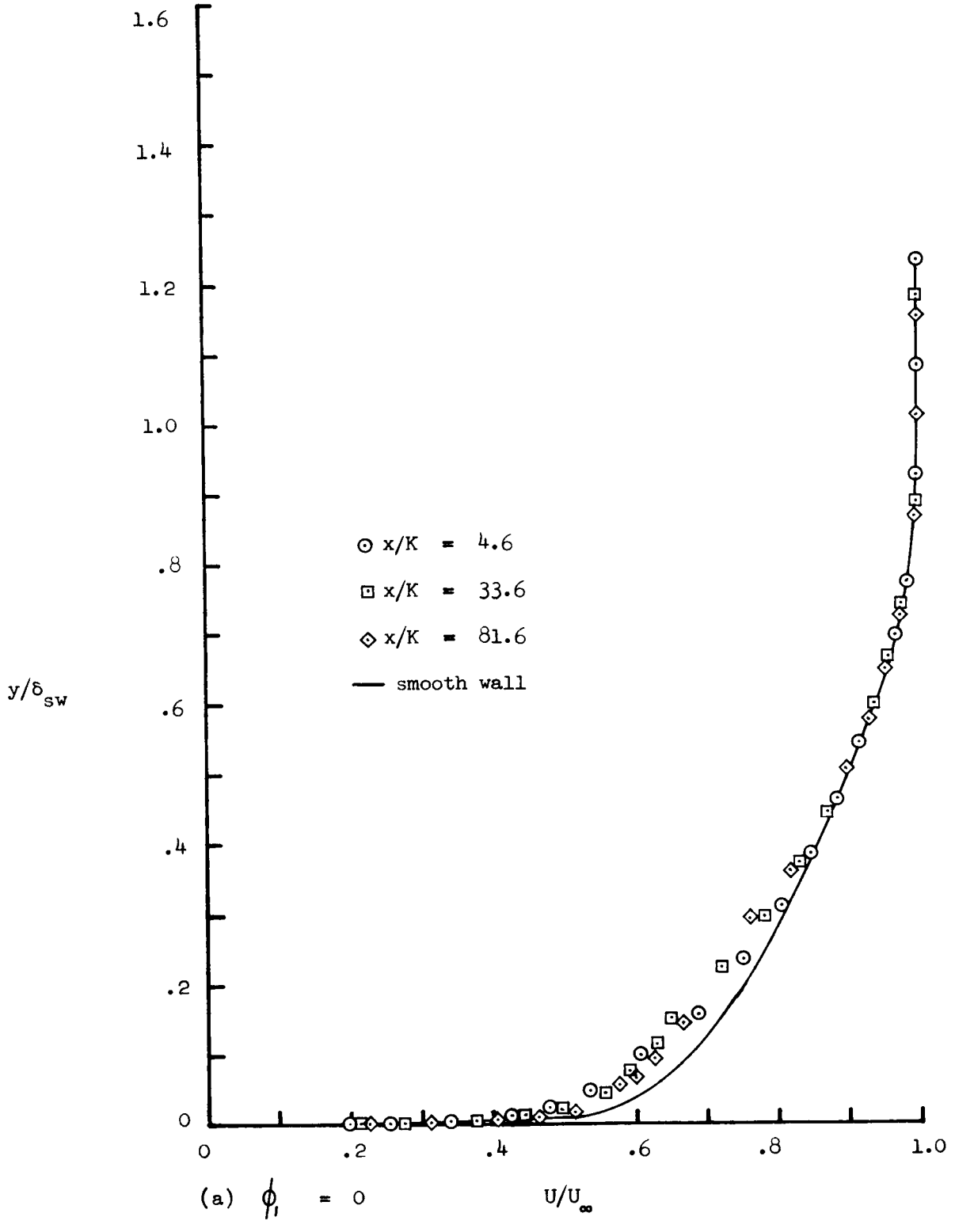

Figure 11 Longitudinal variation of boundary layer velocity profiles downstream of 0.25 - inch elements.

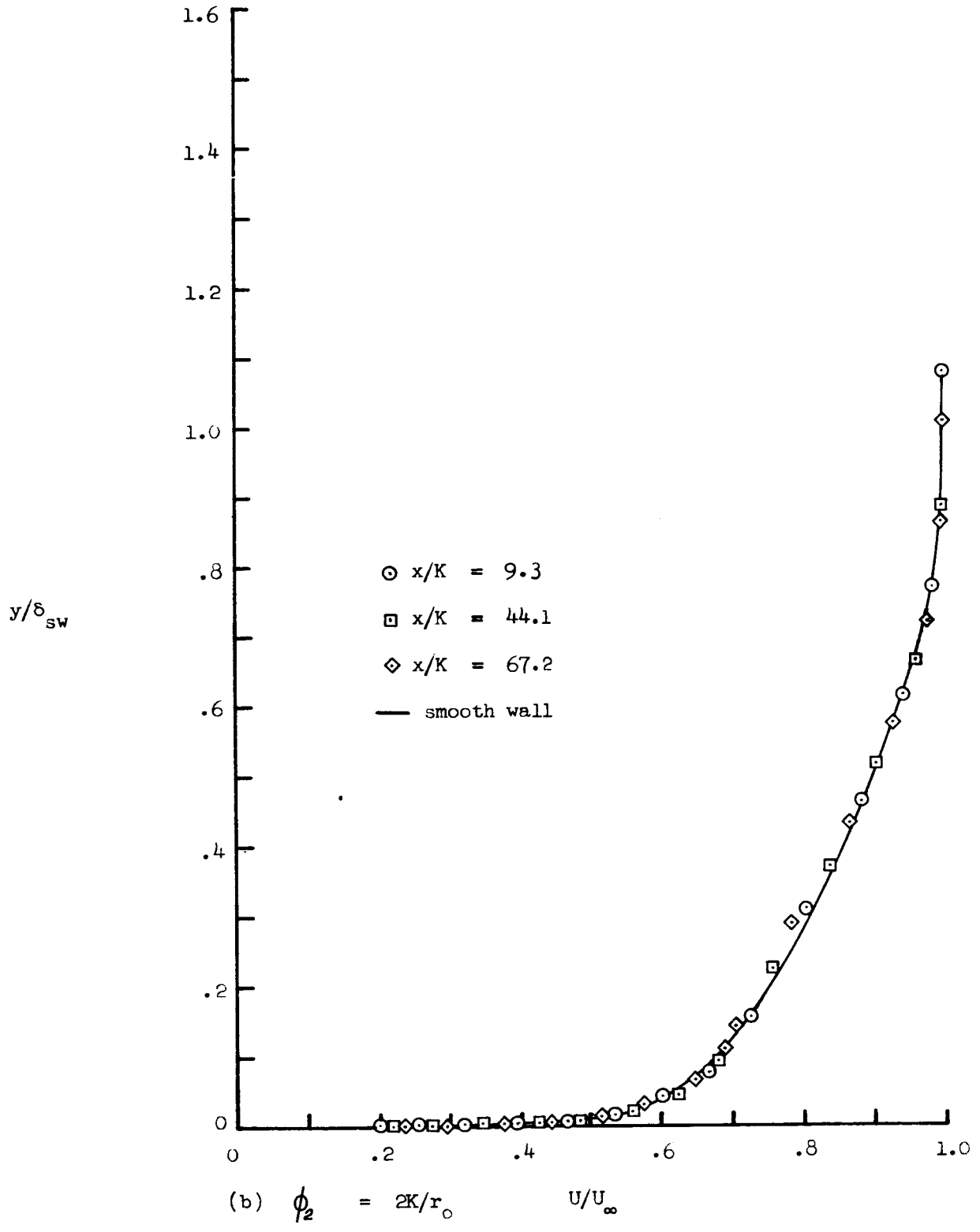

Figure 11 (Continued) Longitudinal variation of boundary layer velocity profiles downstream of 0.25 - inch elements.

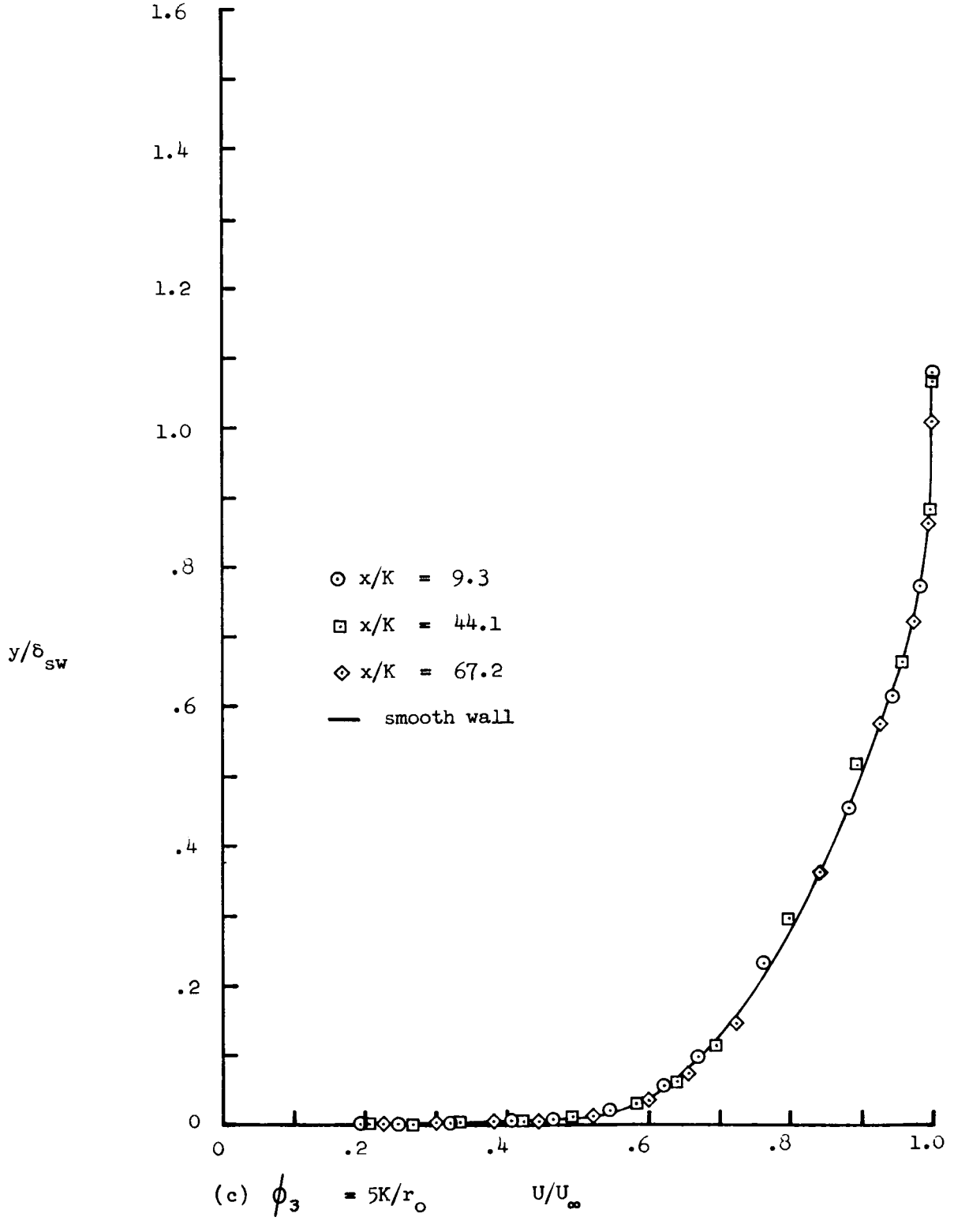

Figure 11 (Concluded) Longitudinal variation of boundary layer velocity profiles downstream of 0.25 - inch elements.

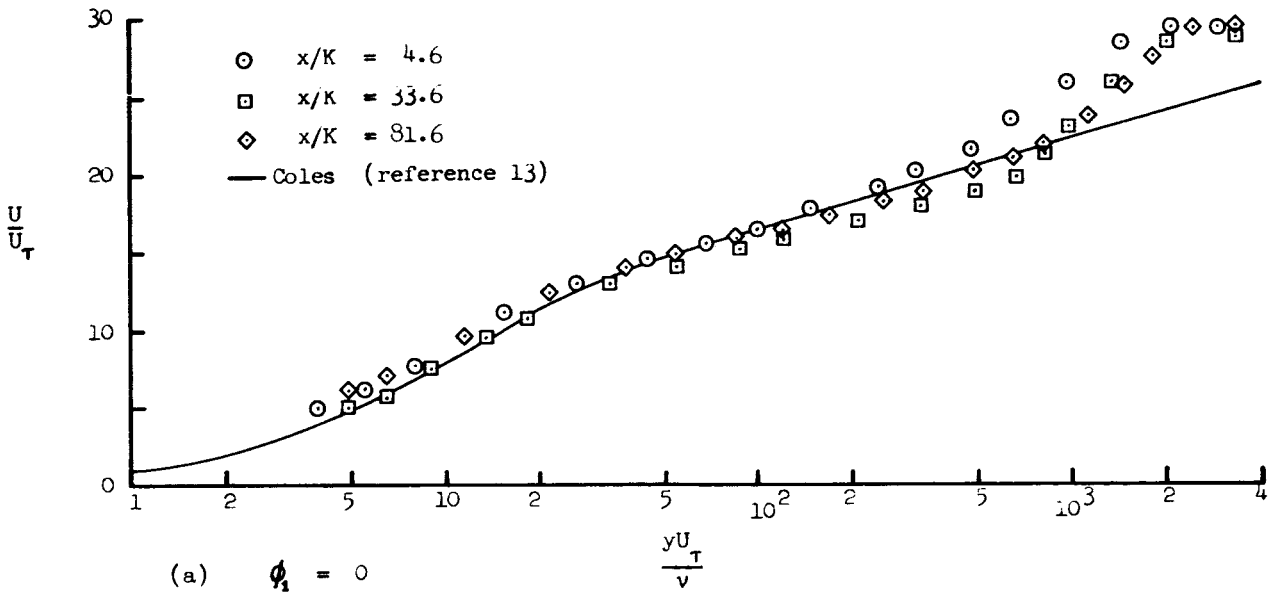

(a) $\phi_1 = 0$

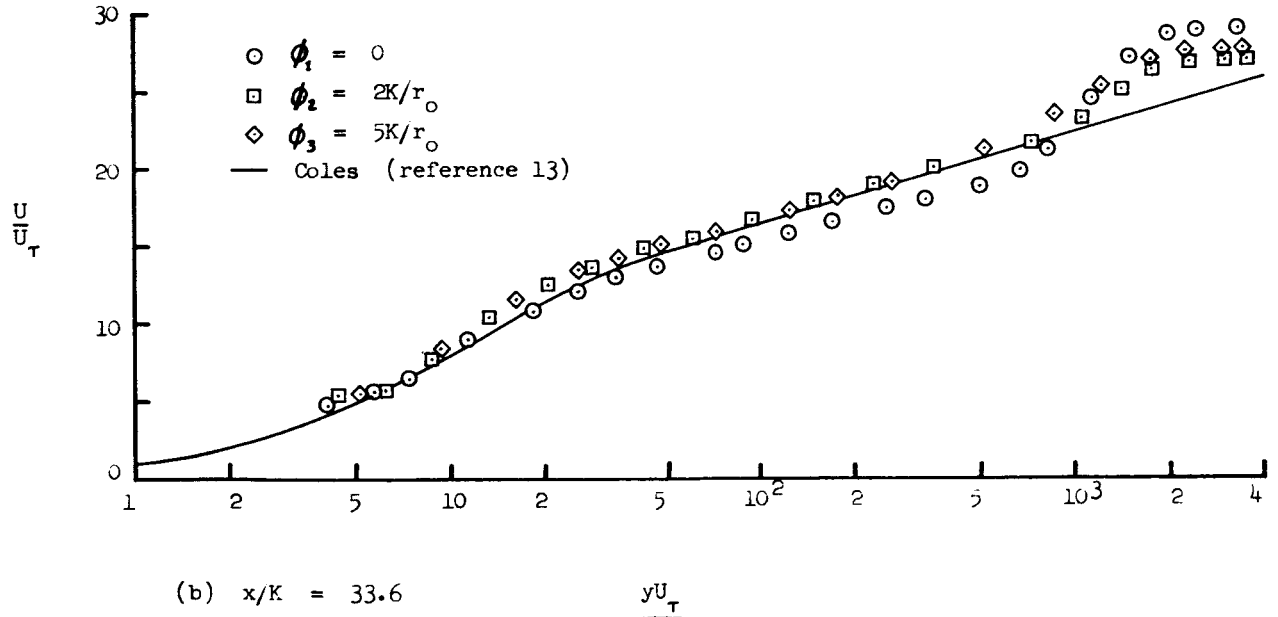

(b) x/K = 33.6

Figure 12 Law of the wall velocity profiles for 0.50 - inch elements.

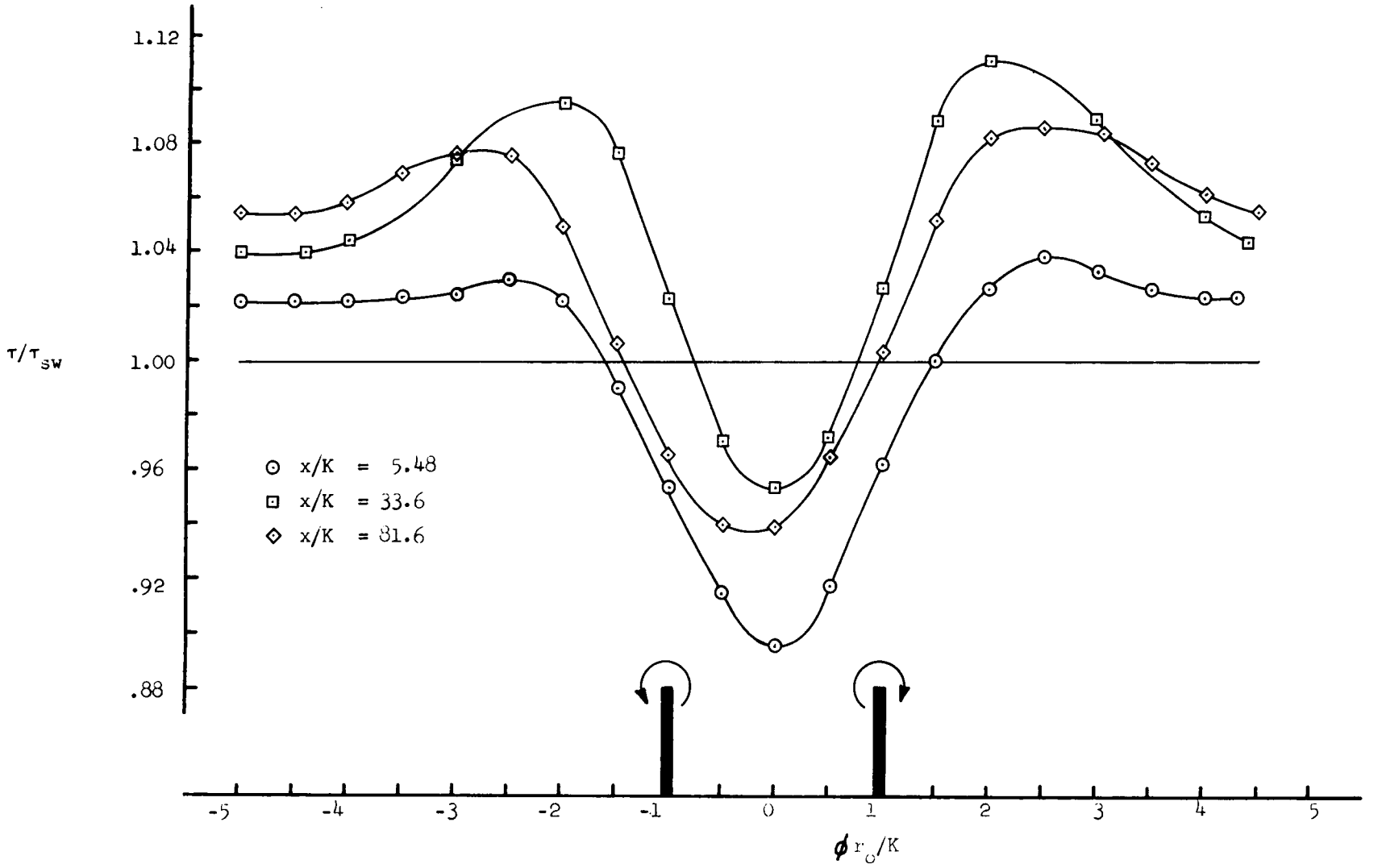

Figure 13 Transverse variation of wall shear stress for 0.50 - inch elements.

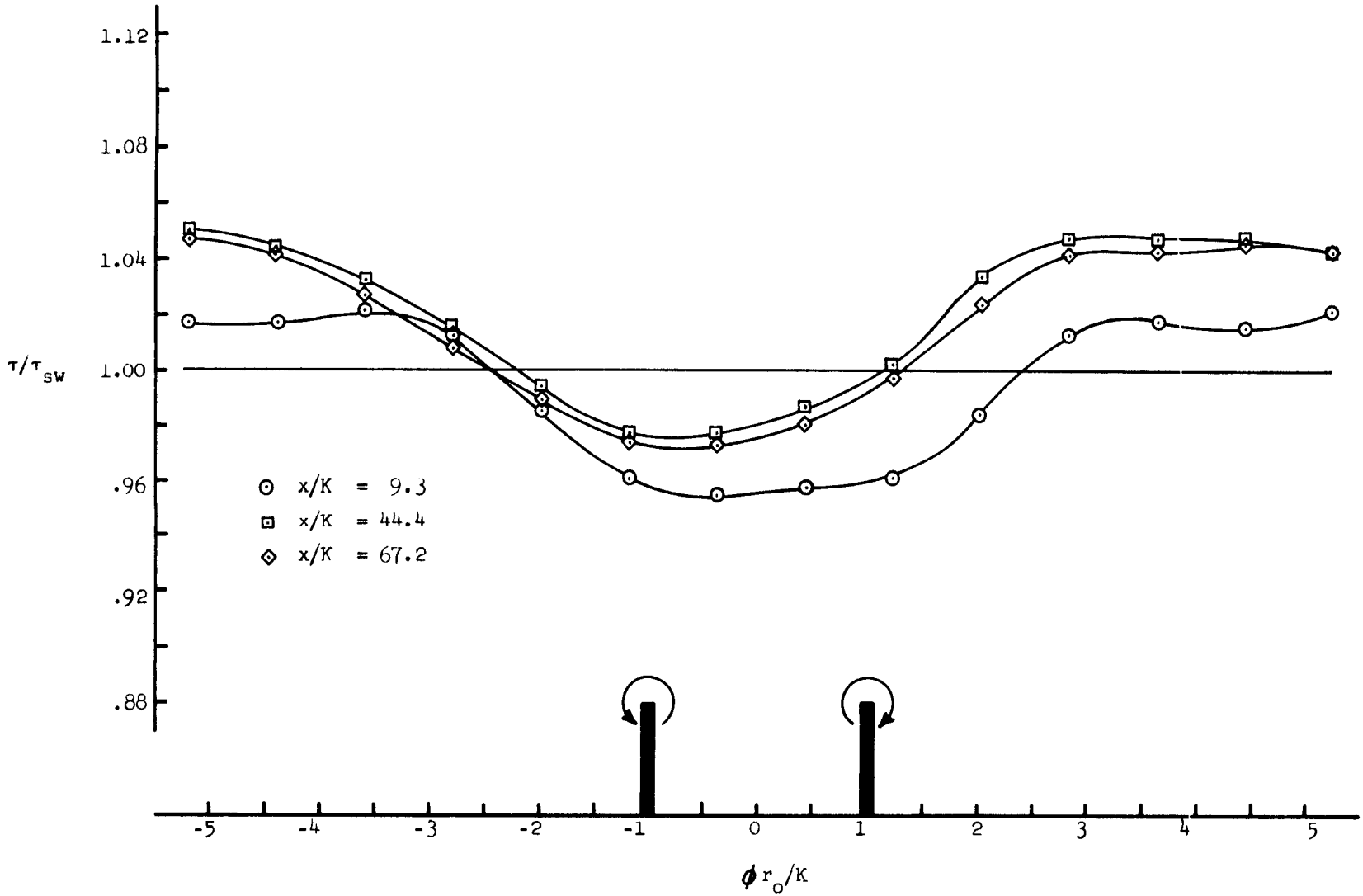

Figure 14 Transverse variation of wall shear stress for 0.25 - inch elements.

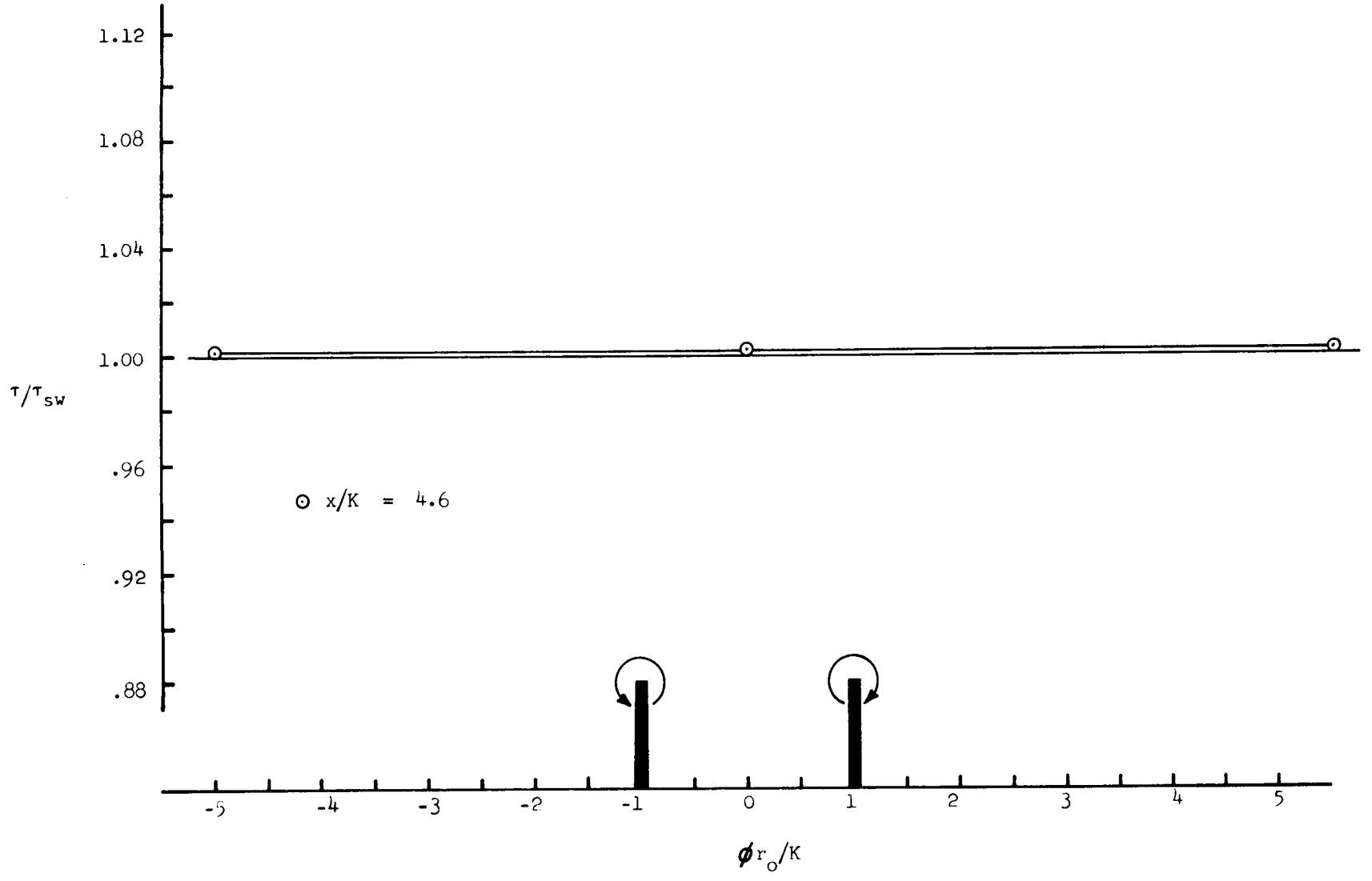

Figure 15 Transverse variation of wall shear stress for 0.05 - inch elements.

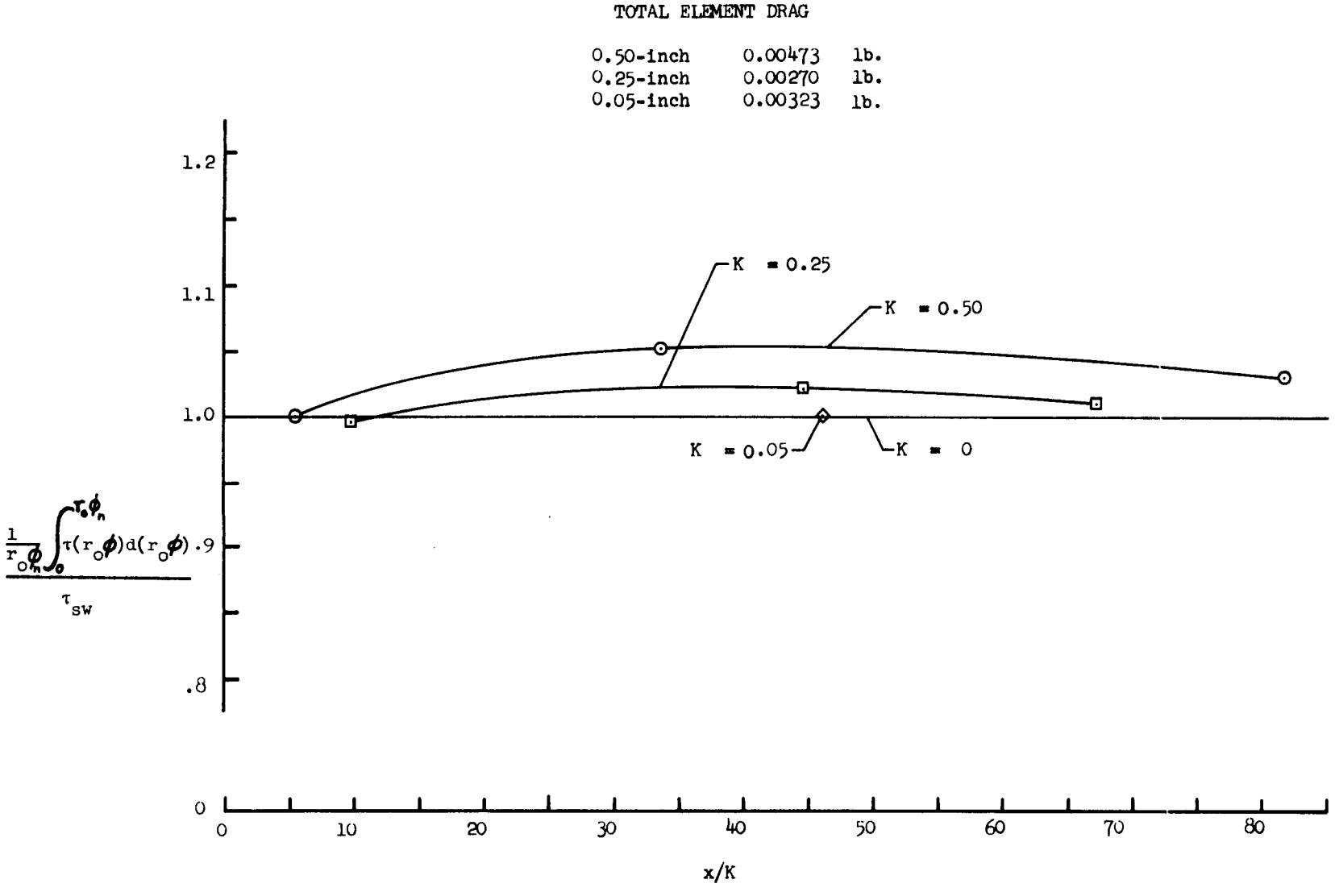

Figure 16 Longitudinal variation of average wall shear stress.

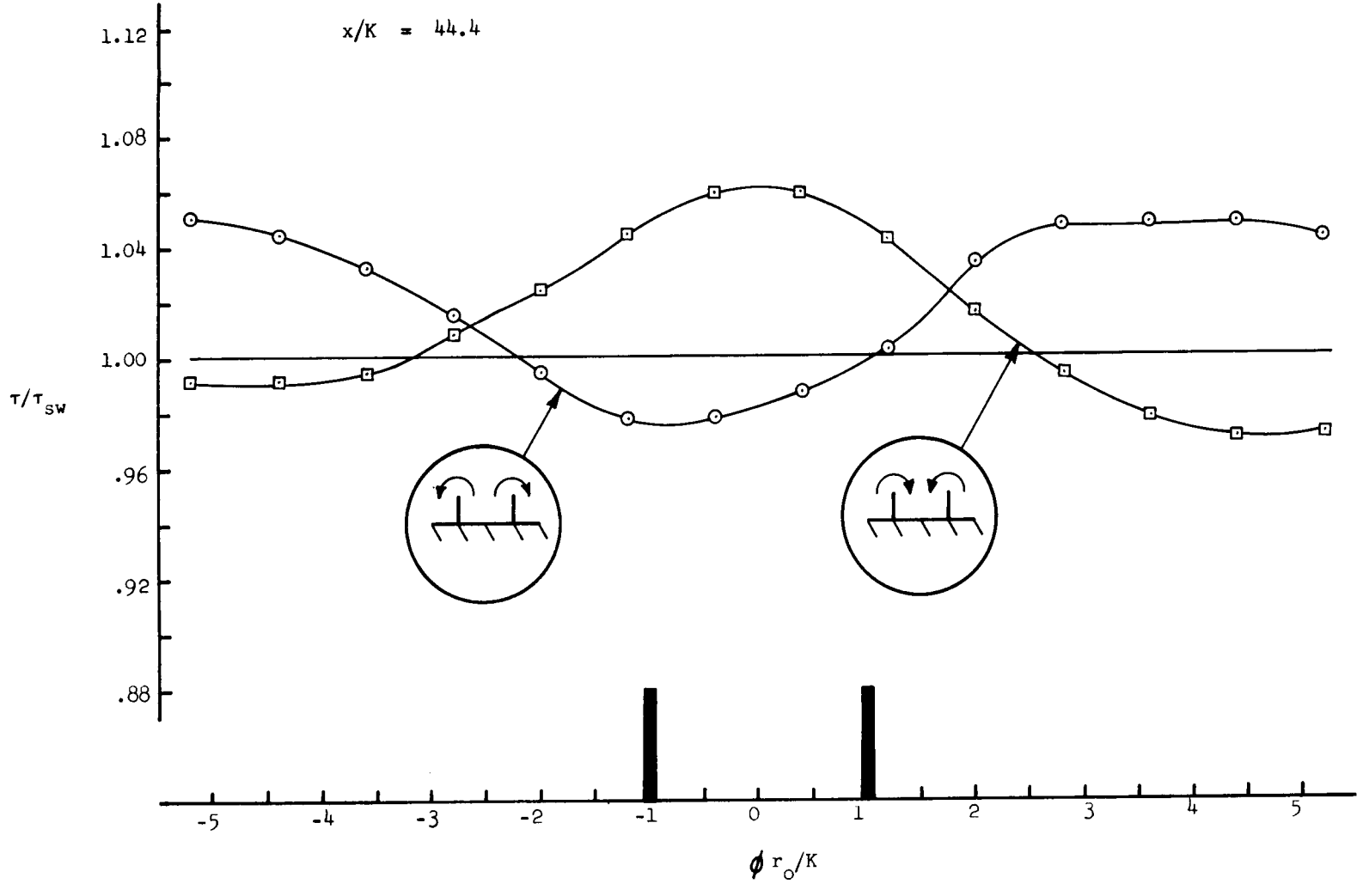

Figure 17 Effect of vortex rotational direction on wall shear stress distribution for 0.25 - inch elements.

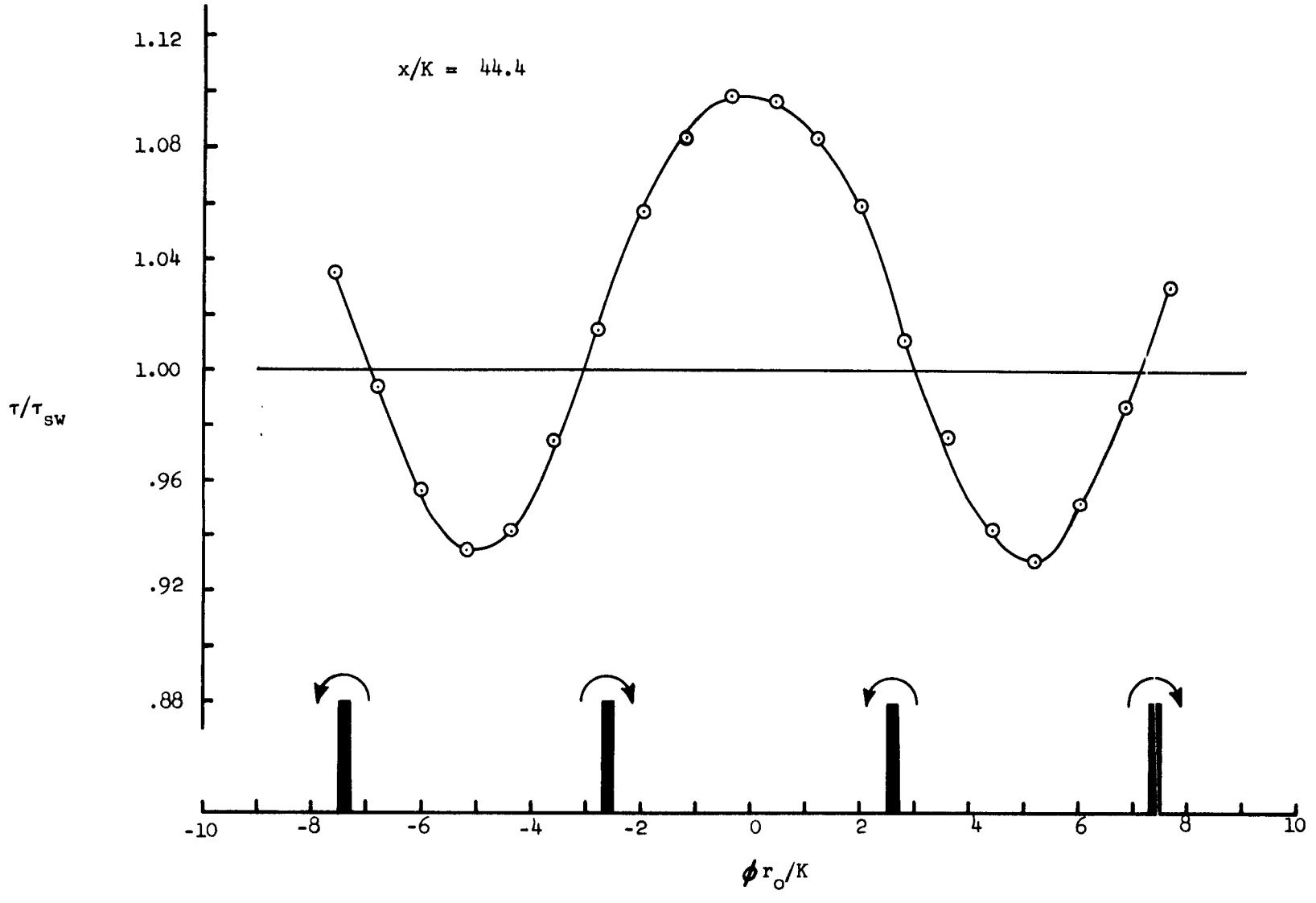

Figure 18 Effect of spacing change on wall shear stress distribution for 0.25 - inch elements.